Received: 18 June 2020 | Revised: 13 February 2021 | Accepted: 12 March 2021

DOI: 10.1002/hyp.14139

WILDFIRE AND HYDROLOGICAL PROCESSES

WILEY

Spatial simulation of forest road effects on hydrology and soil erosion after a wildfire

Longxi Cao[1,2] | William Elliot[2] | Jonathan W. Long[3]

[1]College of Ecology and Environment, Chengdu University of Technology, Chengdu, China

[2]Air, Water, and Aquatic Environments Program, USDA Forest Service, Rocky Mountain Research Station, Moscow, Idaho, USA

[3]Conservation and Biodiversity Program, USDA Forest Service, Pacific Southwest Research Station, Davis, California, USA

Correspondence
Email: welliot@moscow.com

Funding information
China Scholarship Council, Grant/Award Number: Project 201604910077; National Natural Science Foundation of China, Grant/Award Number: Project 41571273 and 41807077; Southern Nevada Public Land Management Act

Abstract

Post-fire catchment and water utility managers throughout the world use predictive models to estimate potential erosion risks to aid in evaluating downstream impacts of increased runoff and erosion, and to target critical areas within a fire for applying mitigation practices. Erosion prediction can be complicated by forest road networks. Using novel GIS technology and soil erosion modelling, this study evaluated the effect of roads on surface runoff, erosion and sediment yields following a wildfire and determined that the predictive models were providing reasonable results. The GeoWEPP model was used to simulate onsite erosion and offsite sediment delivery before and after fire disturbance using a 2-m resolution DEM as the terrain layer. Erosion rates in excess of 4 Mg ha^{-1} year^{-1} were predicted mainly from steep moderate and high severity burn areas. Roads influenced surface runoff flow path distributions and sub-catchment delineations, affecting the spatial distribution of sediment detachment and transport. Roads tended to reduce estimated erosion on slopes below the roads but increases in erosion rates were estimated for road fillslopes. Estimated deposition amounts on roads and in sediment basins were similar to measured amounts. The results confirm that road prisms, culverts and road ditches influence sedimentation processes after wildfire, and they present opportunities to detain eroded sediments.

KEYWORDS
forest roads, soil erosion, watershed, wildfire, WEPP modelling

1 | INTRODUCTION

Soil erosion is one of the major concerns in forest watershed management everywhere. Disturbances such as forest roads, timber harvesting, and fire increase the likelihood of forest soil loss as reported by scientists in Australia (Cornish, 2001; Croke et al., 2005; Lane et al., 2006; Motha et al., 2003; Sheridan et al., 2007; Sheridan & Noske, 2007), North America (Elliot, 2013; Luce & Black, 1999), Europe (Nunes et al., 2018; Shakesby et al., 2016), the Caribbean (Ramos-Scharrón & MacDonald, 2005) and Asia (Akay et al., 2008; Cao et al., 2021; Cuo et al., 2008; Sidle et al., 2004; Y. Zhang et al., 2019; Ziegler et al., 2007). Eroded sediment that is routed to forest streams or lakes can degrade the aquatic environment and impair beneficial uses of surface water resources as reported by scientists around the world (Cole et al., 2020; Elliot, 2013; Elliot et al., 2016; McCormick et al., 2010; Nunes et al., 2018; Ramos-Scharrón & MacDonald, 2005; Smith et al., 2011; Zhai et al., 2014). Roads may accumulate, deliver, or increase sediment in runoff (Gucinski et al., 2001; Sosa-Pérez & MacDonald, 2017; Y. Zhang et al., 2019; Ziegler et al., 2007), increasing the complexity of understanding and evaluating soil erosion and sediment transport processes in post-fire forest conditions.

It is widely reported that fire disturbance in forests usually increases runoff and erosion. This increase is attributed to decreases in soil organic matter (Cole et al., 2020; Ebel, 2012; Kumar et al., 2013; Li et al., 2020: Moody et al., 2013), root mass (Nyman &

Moody, 2012), and ground cover (Cole et al., 2020; Moody et al., 2013). On some soils, there is a tendency for the upper soil layers to become water repellant (Cole et al., 2020; DeBano, 2000; Doerr et al., 2000; Moody et al., 2013; Robichaud et al., 2020; Sheridan et al., 2007; Stavi et al., 2017; Wagenbrenner et al., 2016) increasing surface runoff and erosion. Wildfire usually reduces forest canopy leading to decreased rainfall interception and evapotranspiration, resulting in increased surface and subsurface runoff (Moody et al., 2013; Srivastava et al., 2018); all of which leave the soil more vulnerable to water erosion (Cerdà & Lasanta, 2005; Moody et al., 2013; Robichaud et al., 2010; Srivastava et al., 2018). For several years following a wildfire, the reduction in evapotranspiration due to canopy loss can result in higher soil water content and increases in surface runoff and lateral flow through the soil resulting in increased hillslope and channel erosion (Cole et al., 2020; Srivastava et al., 2018). Soil erosion following severe wildfire can be up to 1000 times greater than before fire as reported by scientists in the USA and Australia (DeBano et al., 1998; Elliot, 2013; Sheridan et al., 2007). At a watershed scale, sediment and runoff response to wildfire are influenced by burn severity and the amount and intensity of precipitation (Robichaud, 2005). An intense rainfall event following a high burn severity fire can greatly increase runoff, erosion and downstream sedimentation (Moody et al., 2013; Robichaud et al., 2000).

Watershed managers rely on hydrologic and erosion prediction tools to support post wildfire mitigation activities (Feikema et al., 2011; Greenbaum et al., 2020; Lopes et al., 2020; Owens et al., 2013; Robichaud, Elliot, et al., 2007; Vieira et al., 2014; Zhai et al., 2014). Building the input databases for these models is time consuming at a time when managers need to make quick decisions about the need for erosion mitigation treatments and evaluating their benefits (Miller et al., 2015, 2016; Robichaud, Elliot, et al., 2007). Satellite imagery is widely used to determine post fire burn severity (Parsons et al., 2010; Robichaud, Lewis, et al., 2007; Robichaud et al., 2020), and that imagery can be combined with climate, soil and topographic data to estimated post fire erosion risk (Lopes et al., 2020; Miller et al., 2016; Robichaud, Elliot, et al., 2007).

Topography is a significant factor in post-fire soil erosion, with longer slopes and steeper slopes generating more sediment (Finkner et al., 1989; Miller et al., 2011). Road construction may change the underlying topography and alter surface hydrology (Gucinski et al., 2001; Reid, 2010; Wemple et al., 2001). Scientists have reported that road networks linked with stream networks may increase stream density within a watershed (Croke & Mockler, 2001; Gucinski et al., 2001; Sidle et al., 2004; Wemple et al., 1996). Forest roads can also decrease the critical gradient for gully initiation and reduce the distance between onsite sediment generation and downstream channels (Katz et al., 2014). Researchers have reported that the road network may also increase watershed peak flow and sediment generation rates (Jones & Grant, 1996; Thomaz et al., 2014). However, road segments can act as hydrological barriers to the natural flow path. Roads with upslope drains intercept hillslope and upstream runoff that can accumulate along road surfaces before drainage through culverts or overtopping of the accumulated runoff across the road surface (Elliot, 2004; Elliot & Tysdal, 1999; Foltz et al., 2009; Gucinski et al., 2001; Sosa-Pérez & MacDonald, 2017; Wemple et al., 2017). Therefore, flow accumulation and flow energy may be redistributed on hillslopes below road segments. This redistribution of runoff can result in altering surface soil erosion and sediment transport processes (Elliot & Tysdal, 1999; Lane et al., 2006; Takken et al., 2008; Zhang et al., 2019).

With the aid of GIS technology and advanced modelling methods, researchers have addressed the influence of road networks on watershed scale hydrology and sediment processes (Akay et al., 2008; Araujo et al., 2014; Brooks et al., 2006; Grace III, 2017; Parsakhoo et al., 2014; Soulis et al., 2014). Most of these researchers stated that road networks will likely accelerate runoff accumulation processes and increase peak flow and sediment generation in otherwise undisturbed forest watersheds. In dry forests, such as the western USA, Australia, and the Mediterranean region, it is only after forest fires that large amounts of sediment are generated from the forested hillslopes. (Elliot, 2013). In these drier forests, roads are usually the main source of upland sediment in the absence of prescribed or wildfire (Elliot, 2013; Grace III, 2017). In addition, a road segment may intercept sediment flux from disturbed areas and become a site for deposition (MacDonald & Coe, 2008; Sosa-Pérez & MacDonald, 2017; Wemple et al., 2001), or enhance runoff, and be a site for additional erosion (Sosa-Pérez & MacDonald, 2017). In wetter forests, such as in the eastern USA and Northern Europe, large storm events can trigger erosion in forests that have not been burned, and roads may influence the fate of such sediment, as was observed by Grace III (2017) when forest runoff from a large storm overwhelmed one of his plots on a road erosion study. Whether the upland sediment is deposited or delivered from the road will depend on the runoff rate, road gradient and design (inslope, outsloped or crowned). A road network effect on surface hydrology is difficult to evaluate spatially as road topography cannot be precisely measured using a coarse DEM. However, a high-resolution LiDAR (Light Detection and Ranging) DEM can capture the topographical details for a more precise hydrologic analyses (Persendt & Gomez, 2016; Sosa-Pérez & MacDonald, 2017; Yang et al., 2014) making it possible to better characterize how road segments can influence surface runoff and sediment transport in a montane watershed.

Numerous models have been developed that have the capability of estimating post-fire and road network erosion. However, validation studies of post-fire hydrologic models' performances are limited (Lopes et al., 2020), and there are no studies using computer modelling to estimate the impact of roads on post-fire erosion processes (Sosa-Pérez & MacDonald, 2017). There is a need for studies in watersheds with roads that have immediate post-fire erosion measurements and LiDAR data. Such a serendipitous combination of circumstances occurred following a small wildfire in 2016, as described below. The first two objectives of this study seek to answer the following questions capitalizing on the considerable wealth of information that was available from that 2016 fire: (1) What are the impacts of forest roads within a wildfire perimeter on post fire runoff, erosion and sediment delivery; and (2) From the observed depositions, is it possible to evaluate the accuracy of a post fire runoff and erosion tool? In order to answer these questions, a third objective was necessary, which was to apply advanced GIS and erosion modelling methods to address objectives 1 and 2. The advanced GIS methods included evaluating the roles of critical source area (CSA), flow path length, and landscape belt analysis on post-fire hydrology and erosion.

The results of this study are intended to increase our understanding of how to model the effects of roads in a forested watershed, how road segments influence surface runoff and post-fire sediment transport processes, and whether the predicted sediment deposition rates are similar to observed deposition rates immediately followed a wildfire. The methodologies developed for this study can be applied to evaluating the impacts of roads in watersheds for not only post fire conditions, but for any land cover where managers are trying to evaluate the watershed effects of roads. Approaches similar to those we have developed can also be applied to analyze hydrologic and sedimentation processes on other complex topography such as terraces (Flanagan & Livingston, 1995) or construction sites (Laflen et al., 2001).

2 | MATERIALS AND METHODS

2.1 | The Water Erosion Prediction Project (WEPP) model

The Water Erosion Prediction Project (WEPP) model is a U.S. interagency model that was developed for applications to croplands, rangelands, and forests (Flanagan & Nearing, 1995; Laflen et al., 1997). It can be run for individual hillslopes or for watersheds made up of hillslope, channel, and channel impoundment elements. The WEPP model mathematically describes the dominant processes that cause surface erosion by water. Flanagan and Nearing (1995) describe how WEPP predicts daily plant growth and senescence, litter accumulation and decay, and canopy and ground cover dynamics. WEPP does a daily water balance and differentiates between rainfall and snow accumulation and melt. When there is a rainfall or snowmelt event, WEPP estimates the runoff using the Green-Ampt infiltration equation for infiltration excess runoff or predicts runoff from rainfall or snowmelt when the soil profile is saturated. If there is runoff, WEPP estimates rill erosion using an excess hydraulic shear model, and interrill erosion as a function of rainfall intensity and runoff rate. In rills on hillslopes or in channels, WEPP estimates sediment detachment, transport, deposition and delivery as functions of hydraulic shear (Flanagan & Nearing, 1995).

A number of interfaces have been developed for the WEPP model, or it can be run from MS DOS commands with no interface. The most utilitarian interface is in Microsoft Windows with a typical WEPP run requiring more than 400 input variables. A WEPP hillslope can be divided into "overland flow elements" (ofes) with unique soil and/or vegetation properties for each element, such as a burned hillslope intersected by a road, or a hillslope with a high severity burn on the upper slopes, and a lower severity burn on the footslopes. The range of outputs from WEPP windows include daily vegetation and hydrologic conditions, and the distribution of erosion for 100 points within each ofe. Runoff and erosion can be viewed by event, annual total, or average annual values from runs that can be for up to 999 years.

Elliot and Hall (2010) have published several online interfaces for WEPP applications to forest and rangeland hillslopes that require minimal user inputs to direct the interface to access online databases for soils, vegetation and climate inputs (Elliot, 2004). These have been very popular with the USDA Forest Service and other land management agencies, completing tens of thousands of WEPP runs annually. The forest and rangeland erosion interface is "Disturbed WEPP", and the soil database for it was last updated in 2014. Other interfaces include "WEPP:Road" for road erosion and sediment delivery analysis, and the Erosion Risk Management Tool "ERMiT" for estimating post-fire sediment delivery and erosion mitigation effectiveness on forest and rangeland hillslopes that have been burned (Robichaud, Elliot, et al., 2007). The Elliot and Hall (2010) database has only two categories for fire, "Low Severity" and "High Severity". The "High Severity" fire is intended to be selected when the soils are found to be water repellent following the fire, and the "Low Severity" when they are not water repellent. A "Moderate" severity fire is one in which the soil is "Low Severity", but the ground cover is in the range of 40%–70%. A "low severity" fire would be modelled with a "Low Severity" soil and a ground cover greater than 70%.

GIS applications for the WEPP model, GeoWEPP for ArcGIS (Flanagan et al., 2013) and QWEPP for QGIS (Milller et al., 2019), define hillslopes and channels from a digital elevation model (DEM), distribute the soil and land use on the hillslopes, and build input files for the WEPP watershed version. With input files from the GIS applications, the WEPP watershed version estimates runoff and sediment delivery from all hillslopes, and then routes hillslope runoff and sediment delivery, and shallow lateral flow through a stream channel network for each event. The model then estimates sediment detachment, transport, deposition and delivery for each channel segment. Preparing soil and management layers for the GIS applications can be time consuming, requiring several weeks. To minimize the time required for file preparation in a post-wildfire application an online database has been developed for the USA to provide post wildfire watershed managers with a suite of GIS files with the same GIS projection as the burned area reflectance classification map or soil burn severity map describing soil, land cover and topography, all formatted at a 30-m resolution for the WEPP model GIS interfaces GeoWEPP or QWEPP (Miller et al., 2015, 2016; Milller et al., 2019). The soil erodibility properties provided by the Miller et al. (2015) and Milller et al. (2019) server are similar to the Elliot and Hall (2010) database for forest and rangeland soils. Miller et al. (2015) and Milller et al. (2019) downloads also include the 30-m U.S. Geological Survey digital elevation model and land use layers, and data from the USDA Natural Resource Conservation Service (NRCS) soil survey. To utilize the Miller et al. (2015) and Milller et al. (2019) database, the user uploads the burn severity map or burned area reflectance category map to the Miller et al. site, and within a few minutes downloads the soil, land use and DEM files.

The soil files have merged the NRCS soil profiles with the WEPP soil erodibility values for each of the burn severities. Lew et al. (2020) have developed online GIS interfaces that combine the GIS tools of GeoWEPP/QGIS with the Miller et al. (2015) and Milller et al. (2019) databases. Lew et al. (2020) applications, however, lack flexibility in climate selection and DEM resolution, and in incorporating other advanced topographical analyses or visualization options offered by ArcGIS or QGIS.

When using GeoWEPP and most other watershed GIS tools, the first step in a watershed analysis is to carry out several GIS topographic operations to delineate the hillslopes and channels by defining a "critical source area" (CSA) (Flanagan et al., 2013). The CSA is the pixel flow path value that must be exceeded before a given pixel can be defined as a "channel" pixel. Once the channel pixels have been identified, sub watershed or hillslope polygons can be defined for further runoff and erosion modelling (Flanagan et al., 2013). The GeoWEPP and QWEPP GIS applications can be run in two modes, "watershed" and "flowpath" (Flanagan et al., 2013). When running in watershed mode, GeoWEPP lumps the shallow lateral flow, surface runoff and erosion response for each 2- to 10-ha hillslope polygon delineated by the model, and then routes the runoff and sediment through the stream network for each storm. The output from a GeoWEPP "watershed" run is sediment loss and runoff for each hillslope polygon and channel segment. In the "flowpath" mode GeoWEPP and QWEPP estimate the erosion for each pixel in the GIS, considering the slope steepness, landscape position, soil properties and land cover for each pixel. Each individual flowpath ends with a pixel adjacent to the channel and follows the flowpath up to the ridge from that pixel, draining an area of 0.2 to 0.5 ha. Flowpath "length" is increased to account for converging flowpaths on the landscape. The flowpath method was developed to show the distribution of erosion or deposition on the landscape and was not intended to be used to predict sediment delivery (Flanagan et al., 2013). The output from a flowpath run will also include an average erosion rate for each hillslope polygon. The "flowpaths" as defined by GeoWEPP and QWEPP are not the same as the flow path lengths as defined by the ArcMap Spatial Analyst for routing runoff as described later, although the GIS steps in their derivation are similar, they are not identical (Flanagan et al., 2013; http://desktop.arcgis.com/en/arcmap/).

The WEPP Model MS Windows interface can output details of erosion distribution along a hillslope profile as well as other details about temporal and spatial hydrologic and erosion processes (Flanagan & Livingston, 1995). Within the Windows interface for the Watershed version of WEPP, channel structures such as sediment basin size and shape and spillway dimensions can be described in detail (Flanagan & Livingston, 1995). The output for a channel structure includes how many times the structure was filled with sediment during the simulation run.

Elliot et al. (2000) state that because of the high natural variability of forest soils, particularly after a fire, "The accuracy of a predicted runoff or erosion rate is, at best, plus or minus 50%" for a WEPP application for forest and rangeland erosion prediction. For predictions of erosion on burned forest hillslopes, Robichaud, Elliot, et al. (2007) have incorporated this variability into post fire erosion estimates in the ERMiT application of the WEPP model. The ERMiT output is the sediment delivery that may be exceeded for a given probability, having considered variability in soils, ground cover, and climate and spatial variability in burn severity.

2.2 | Study site description

Lake Tahoe is an extraordinarily large (500 km^2), deep (500 m), and clear lake at an elevation of 1890 m above sea level. It is on the eastern slopes of the Sierra Nevada Mountains on the California-Nevada, USA border with (Figure 1). Stakeholders within the Tahoe Basin are keen to maintain the lake's clarity (Nevada Division of Environmental Protection, 2011; Water Boards and NDEP, 2008). Watershed analyses carried out in the basin have identified urban development and the road network in forested areas as major sources of sediment (Water Boards and NDEP, 2008). The WEPP model (Flanagan et al., 2013; Laflen et al., 1997) was applied to a number of watersheds within the Tahoe Basin to better understand the role of forests and forest management in hydrologic and erosion processes (Brooks et al., 2016). The study found that underlying geology, weather patterns and vegetation cover were all important factors influencing surface runoff, subsurface flows, and both upland and channel erosion. In 2016, a group of public agency and non-government organizations formed the Lake Tahoe West Restoration Project to focus on developing methods to reduce wildfire risk on the Western Slopes of the Lake Tahoe Basin while causing minimal impact on hydrology and water quality (https://www.nationalforests.org). The project chose to use the WEPP model to provide hydrologic and erosion modelling to support their overall analysis because of the previous modelling of Brooks et al. (2016) in demonstrating the utility of WEPP in the Tahoe Basin. The results of this expanded study included the distribution of current erosion by approximately 10-ha hillslopes on the western slopes of the basin (Lew et al., 2020). The runoff and sediment delivery predictions for current conditions were validated for several watersheds in the study area that had streamflow and sediment monitoring data, and the modelling then expanded to cover all watersheds in the project area. Runoff and erosion were then estimated should the watersheds be thinned, treated with prescribed fire, or subjected to wildfire (Lew et al., 2020). As with the Brooks et al. (2016) study, the WEPP-estimated runoff and sediment delivery amounts for the undisturbed condition were similar to observed values. However, the accuracy of runoff and sediment estimates following the projected wildfire could not be validated as there had been no wildfires in the gauged watersheds on the restoration project landscape.

Early in the morning on 14 October, 2016, a small wildfire subsequently named the "Emerald Fire" occurred on the southwest side of the Lake Tahoe Basin (Figure 1), Latitude 38.94°N, Longitude 120.08°W. Fueled by high winds (gusting up to 89 $km\ h^{-1}$), burning 71 ha (Figure 1, red boundary) by the following morning, when rainfall extinguished the fire. Precipitation depths of 81, 56 and 114 mm were recorded at the nearby Echo Peak SnoTel Site 10 km south of the fire

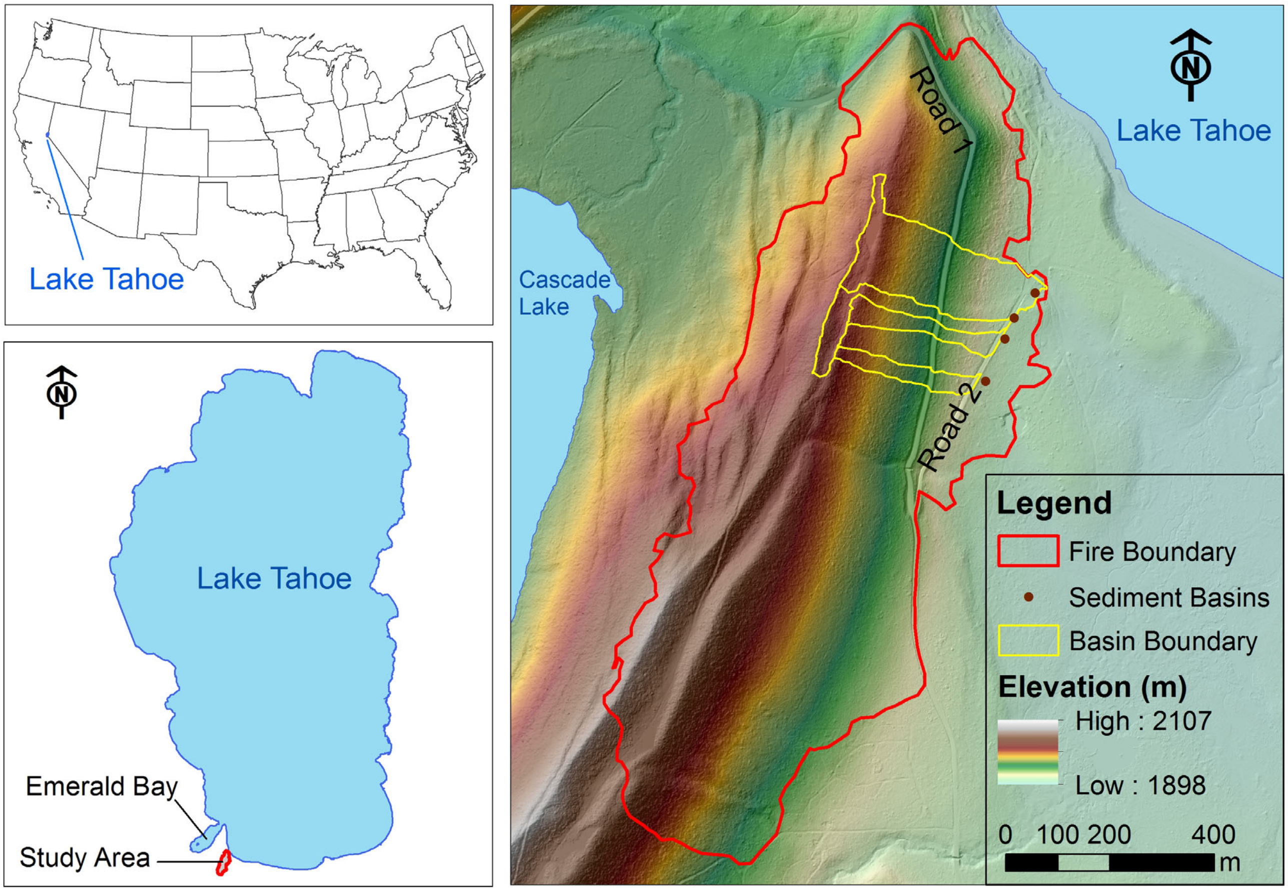

FIGURE 1 The location of the 2016 Emerald Fire study site with topography based on a 2-m LiDAR DEM. The fire boundary is outlined in red. The four sediment basin locations are shown by black dots, and their watersheds are outlined in yellow

on October 14, 15 and 16, respectively. (NRCS, 2020). Highway 89, an asphalt-surfaced two-lane highway (Figure 1, Road 1) and a gravelled private road (Figure 1, Cascade Road or Road 2) pass through the northeast part of the burn site. According to our field survey, road 1 is paved and flat without drains with the gradient of about 4% (2.3°). Road 2 is gravelled and crowned with drains on both sides, and a gradient of about 7% (4.0°). The burned area above and between the roads has a generally uniform gradient averaging about 40% (21.8°). The average gradient of hillslope below road 2 is about 17% (9.6°). There are 4 sediment basins installed to trap road sediment below road 2 (Figure 1). The areas of the contributing sediment basin sub-catchments are 0.9, 1.05, 1.38 and 4.1 ha, moving left to right on Figure 1. The lengths of the sub-catchments from the sediment basins to the ridge ranged from 300 to 350 m.

From the three rainfall events, more than 200 Mg of sediment were deposited on Road 1, (Figure 1; Vollmer, 2016). Eldorado County had to empty four sediment basins beside Road 2, removing an estimated 134 m^3 (about 120 Mg) (Personal Communication, R. Wigart, Stormwater Coordinator for the Tahoe Basin, Eldorado County, California, 13 December 2016). The USDA Forest Service estimated the upland erosion following this wildfire with the ERMiT model as is a common practice within the agency (Robichaud, Elliot, et al., 2007; Young, 2016). The post-fire impacts report was completed 12 days later (Young, 2016). Typically, a soil burn severity map is generated for wildfires from satellite data as described below, and then verified with a site visit (Parsons et al., 2010; Robichaud, Lewis, et al., 2007). For this small fire, however, a burn severity map was not created. The assessment was done remotely by request, and Young (2016) did not visit the site. Young's post-fire assessment assumed that the soil burn severity was moderate throughout (Young, 2016).

In the Tahoe Basin vegetation is comprised of mixed conifer forest with significant areas covered by meadows, riparian areas, or bare granite outcrops (Coats et al., 2008; Nevada Division of Environmental Protection, 2011). The climate is comprised of wet winters and dry summers (Csb according to the Köppen classification; Ackerman, 1941). Average annual precipitation at the Echo Peak SnoTel station located 10 km south of the site is 1496 mm (NRCS, 2020). Site hydrology is dominated by rain-on-snow events (Brooks et al., 2016). Soil textures within the study area are dominated by a "gravelly loam coarse sand" derived from decomposed granite (Brooks et al., 2016; Lew et al., 2020; USDA, 2007). For WEPP Modelling purposes, the soil was assumed to be the "sandy loam" in the WEPP soil databases.

Following the Emerald Fire, as part of ongoing watershed modelling studies within the Tahoe Basin, the authors prepared a surface erosion and mass wasting report for stakeholders in the Tahoe Basin

(Elliot, Cao, et al., 2018) evaluating the Young (2016) report, and in support of the Lew et al. (2020) watershed management project. In support of that study, the authors visited the site on 3 August, 2017, to evaluate ground cover, measure sediment basin volumes, and become more familiar with the site. During the site visit, we noted that the ground cover on the upper part of the fire that was classified as high severity was about 45%, much of which was due to needle cast in the months following the fire. On the lower part of the fire that was classified as low severity ground cover was 100% over much of the area as there was a considerable amount of unburned organic material plus additional needle cast from the partially burned forest canopy. During previous visits to the basin, steep south facing slopes were observed to have some bare soil exposed, whereas lower gradient sites tended to have a complete ground cover of partially burned or unburned organic material. We used conservative lower ground cover values for the analysis as shown in Table 1 to minimize the risk of under predicting erosion rates.

2.3 | Data collection and preparation

LiDAR terrain data were used to define flow paths and delineate the topography of roads in the study site. The LiDAR remote sensing data for Lake Tahoe were collected by Watershed Sciences, Inc. (WSI) in August 2010. The survey used two Leica ALS50 Phase II laser systems mounted in a Cessna Caravan 208B. The average first-return density of the delivered dataset was 11.82 points m^{-2} and the average ground return density was 2.26 points m^{-2}. A raster elevation data set with a resolution of 0.5 m was created based on the ground return points from the LiDAR flight (Figure 1).

We estimated soil burn severity using the differenced Normalized Burn Ratio (dNBR) from Landsat ETM 7 images from information before (24 September 2016) and after (18 October 2016) the fire to generate a Burned Area Reflectance Classification (BARC) layer at a 30-m resolution (Figure 2; Parsons et al., 2010; Robichaud, Lewis, et al., 2007). The BARC data were classified following Parsons et al. (2010) to estimate soil burn severity (Table 2) resulting in the soil burn severity map (Figure 2).

We uploaded the soil burn severity map to the Miller et al. (2015) main web page, and then downloaded topography, soil and land use files at a 30-m resolution formatted for input for GeoWEPP (Miller et al., 2015, 2016) for the study site. The LANDFIRE Existing Vegetation Type (EVT) data (https://www.landfire.gov/evt.php) were also downloaded from the Miller et al. (2015) site to determine the prefire land cover. The distribution of soil properties (Table 1) and land use data were provided as 30-m resolution raster files and stored in an ASCII format, as GIS layers for both pre-fire and post-fire conditions. The soil properties that were downloaded (Table 1) were not altered for this study as the authors wanted to evaluate how well the model would perform with these standard properties. The soil properties for the roads were obtained from the Elliot and Hall (2010) WEPP:Road online interface.

2.4 | Spatial and hydrological analysis methods

GIS-based spatial analyses and digital terrain analyses, and the GeoWEPP GIS application were adopted to explore the spatial distribution of flow paths and predicted onsite soil loss rates. The Spatial Analyst Tools distributed with ArcGIS 10.3.1 were used evaluate the effects of roads and other terrain features on flow directions, while the "flowpath" mode in GeoWEPP was used to estimate the erosion rate for each pixel. The ArcGIS hydrological analysis tools were applied to determine how the roads impacted sub catchment delineation within the fire boundary, noting whether the catchments were cut off by the roads, or if the overland flowpaths continued over the road. The hydrologic tools were also used to calculate the upstream flow length for each pixel and delineate sub-catchment boundaries. The effect of the CSA on flow path density above and below roads was evaluated within ArcGIS to better understand the effects of road segments on overland flow paths. The CSA is the threshold ArcMap flow accumulation pixel value (https://desktop.arcgis.com/en/arcmap/10.

TABLE 1 WEPP soil erodibility values assumed for GeoWEPP and WEPP windows erosion modelling for the 2016 emerald fire as downloaded from the Miller et al. (2015) online server for unburned and burned soil properties, and Elliot and Hall (2010) for road soil properties. Ground cover was assigned by the authors

	Property				
	Ground cover	Interrill erodibility, K_i	Rill erodibility, K_r	Critical shear τ_c	Effective hydraulic conductivity
Units	Percent	kg s m^{-4}	s m^{-1}	Pa	mm h^{-1}
Land Cover					
Unburned	90	400 000	0.00008	2	60
Low Severity	90	400 000	0.0006	1	25
Mod Severity	45	400 000	0.0006	1	25
High Severity	25	400 000	0.0007	1	16
Gravel Road	0	2 000 000	0.0004	2	10.2
Paved Road	0	5	0.000001	10	0.08

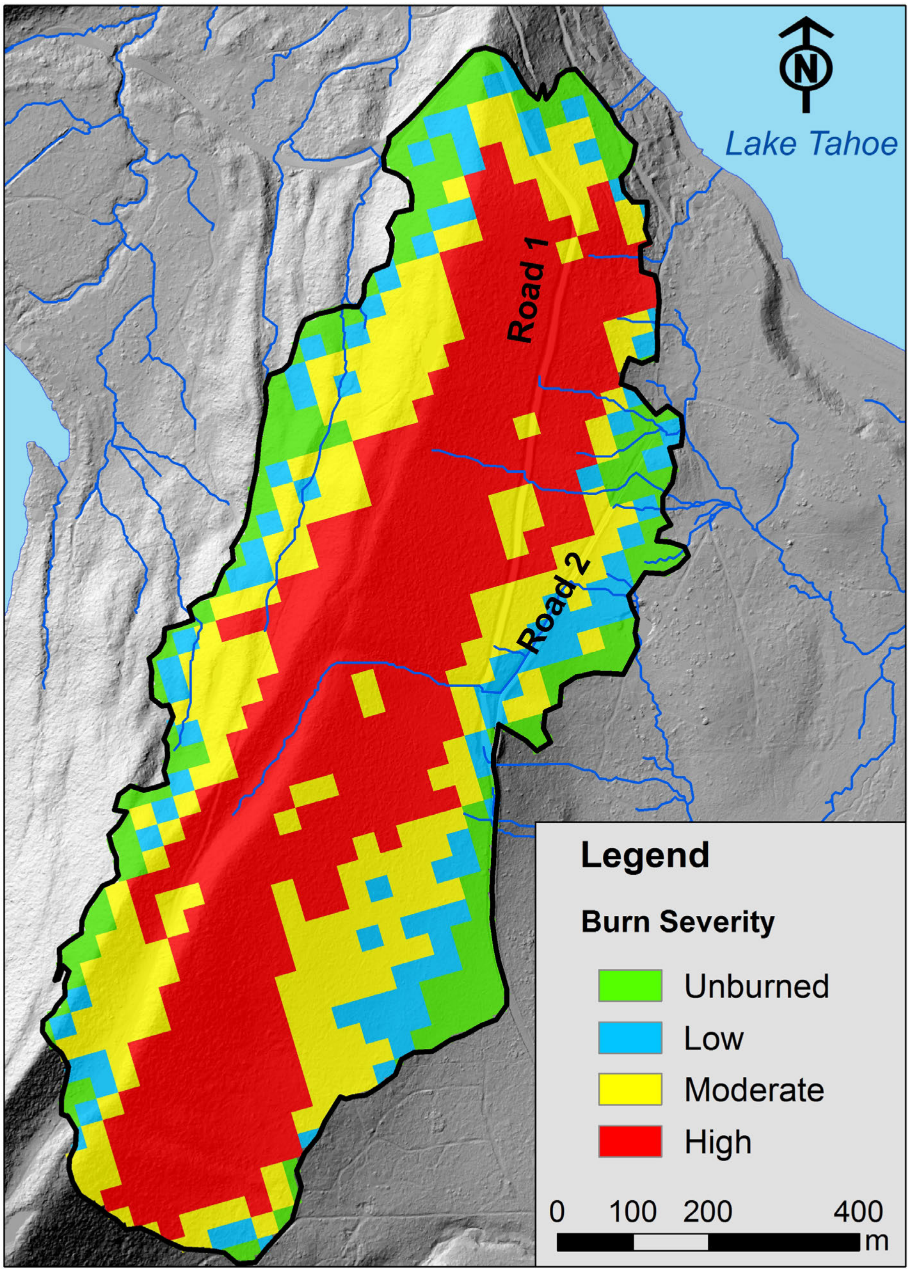

FIGURE 2 Soil burn severity map for the 2016 Emerald Fire derived from 30-m pixel Landsat images from before and after the fire. The blue lines are ephemeral channels. There were no seasonal or perennial streams within the fire perimeter

TABLE 2 Distribution of estimated soil burn severity categories after the 2016 Emerald fire

Burn severity	dNBR range	Area (ha)	Percent (%)
Unburned	≤99	9.43	13.28
Low severity	100–269	8.25	11.62
Moderate severity	270–659	20.65	29.08
High severity	≥660	32.67	46.01

3/tools/spatial-analyst-toolbox/flow-accumulation.htm) that when converted to area must be exceeded to define a channel. To delineate a reasonable channel network, the CSA is generally determined by factors such as local terrain, climate and soil characteristics (Tarboton et al., 1991). Considering are no channels in the study site, the CSA was used to simulate different densities of flow paths rather than extracting real channels. For example, in the case of high intensity storms, relatively small upslope accumulated areas are needed to form concentrated flow paths. Different densities of concentrated flow paths can be delineated by changing the CSA values. For an advanced analysis, CSA values selected were 200, 400 and 1000 m^2. ArcMap flow paths that intersected with the upslope side road edges were recognized as inflow, and outflow paths were those that intersected with road edge on the downslope side. GIS analyses were conducted to demonstrate road segment effect on sub-catchment delineation. Sub-catchment boundaries were determined with a CSA of 0.5 ha. The sub-catchments were then overlaid with the surface topography and road segments to visually evaluate the effects of roads on sub-catchment delineation. To evaluate the effects of the road segments on flow path length, an ArcGIS flowpath analysis was carried out for the 2-m LiDAR DEM, and the same analysis using a 10-m U.S. Geological Survey DEM (https://www.usgs.gov/core-science-systems/ngp/tnm-delivery). The 10-m DEM masks the effects of most road segments on surface topography since road segments are less than 10 m wide.

The ArcGIS Buffer Tool (ESRI, 2016) was applied to generate 10-m-width buffer belts in the downslope direction from the ridge and roads. There were 13 buffer belts below the ridge and 10 belts below each road segment. The burned area was divided into three 100-m belts (above roads, between roads and below roads) using the ESRI (2016) Buffer tool. The 100-m belts were overlaid on the two flowpath layers to determine the average flow path length within each belt, with and without roads. The belts were also used to determine the average erosion rate for all of the pixels within a belt following a post-fire WEPP watershed "flowpath" run.

2.5 | Applying GeoWEPP and WEPP windows

The GeoWEPP model version 10.3 was applied in ArcGIS 10.3.1 for modelling runoff and soil erosion in the Emerald fire area. Topography from the LiDAR layer, and soil and landuse layers from the Miller et al. (2015) database were preprocessed before running the model to ensure the GIS projections were compatible. We determined that the 0.5-m LiDAR DEM would likely generate too many flow paths, exceeding the maximum memory limitation in GeoWEPP running on a PC. Therefore the 0.5-m DEM was resampled as a 2-m DEM with the ArcMap Resample tool using the “Bilinear” method for hydrological process simulation and soil loss prediction. The 30-m resolution soil and landuse data from the Miller et al. (2015) database were also resampled as 2-m raster files to be compatible with the 2-m DEM using the “Nearest” method to maintain consistent pixel values. The original downloaded soil data did not describe the road surface erodibility conditions, so the soil properties for the road surface pixels were manually revised to describe the road for those cells (Table 1).

When applying GeoWEPP to our study area, a CSA of 0.5 ha was necessary in order to generate a channel network to link most of the hillslopes within the Emerald fire area. For some hillslopes that were hydrologically independent from the adjacent areas, the CSA was reduced to 0.3 ha to generate more detailed channels to include these slopes. Offsite sediment yields for both pre-fire and post-fire conditions in the study area were estimated for each of the sub-catchments within the fire perimeter (select “Watershed” as the GeoWEPP simulation method). For the post-fire run, a climate file was built for the year 2016 using the observed daily temperature and precipitation data from the Echo Peak SnoTel station. The pre-fire erosion modelling was carried out using long-term observed weather statistics from the same station to generate a 20-years stochastic climate to get an average annual erosion for the unburned forest conditions (Scheele et al., 2001). A GeoWEPP flow path simulation was carried out to evaluate the effects of road segments on post-fire surface flow accumulation, sediment detachment and sediment transport by pixel. The sub catchment map was overlaid on the flow path erosion map to determine how the catchment-road interaction effected the distribution of erosion on the landscape. Road-related flow paths were extracted for several CSA values and detailed analyses were carried out on the effects of roads on the distribution of predicted erosion rates within the fire perimeter. To evaluate the effect of roads on the distribution of soil loss, a series of 10-m “belts” were established parallel to and above road 1, below road 1, and below road 2 using the ESRI (2016) Buffer tool. The WEPP onsite soil loss rates for the pixels within each ArcMap 10-m buffer belt were averaged to explore the spatial variation in the estimated soil erosion. To estimate deposition on Road 1, 22 hillslope profiles that intersected with the road were generated from the DEM and run in WEPP Windows, resulting in an estimated erosion or deposition rate for 300 points for each profile. The watershed topographies describing each of the sub-catchments above the four sediment basins delineated from the GeoWEPP analysis were imported into the WEPP Windows Watershed version. The measured dimensions of each sediment basin, assuming an “open” or weir type outlet were described in detail in the “Structures” file in the WEPP Windows Watershed Version interface (Flanagan & Livingston, 1995), and the resulting deposition rates for each sediment basin were estimated for the three post fire storms.

3 | RESULTS

During the site visit in August 2017 the total ground cover in the upper part of the fire was 45%, with about 35% due to needle cast that had occurred in the months immediately following the fire. Below road 2, ground cover was greater than 90%. The total volume of the four sediment basins below road 2 was determined to be 79.13 m^3.

The advanced GIS and WEPP modelling techniques provided both visualization and tabular results showing a number of hydrologic and sedimentation impacts of roads on the landscape following a wildfire. The results also show that the rapid response application of the ERMiT model by the Forest Service (Young, 2016) provided reasonable estimates of post fire erosion risk associated for large hydrologic events, and that the post wildfire erosion rates estimated in the Lew et al. (2020) were reasonable.

3.1 | Road segment effect on hydro-geomorphology characteristics

We evaluated the role of the CSA in determining how roads affected flow path density. As the CSA was reduced, the number of flow paths increased and the average distance between flow paths decreased. Table 3 shows that the number of outflow paths from roads is always less than that of the inflow paths. This effect is especially noticeable for the smaller CSAs with more dense flow paths, where a larger portion of inflow paths are intercepted by road segments and result in relatively fewer outflow paths compared to the 1000-m^2 CSA. Road 2, which falls below road 1, showed a lower density of outflow paths

TABLE 3 The effect of critical source area (CSA) on the number and spacing of flow paths above and below roads 1 and 2 (Figure 3) within the 2016 Emerald Fire perimeter

Type of flow paths	Flow path CSA = 1000 m²		Flow path CSA = 400 m²		Flow path CSA = 200 m²	
	Number	DBF (m)	Number	DBF (m)	Number	DBF (m)[a]
Flow into road 1	44	20.91	88	10.45	124	7.42
Flow out of road 1	41	22.44	58	15.86	72	12.78
Flow into road 2	23	20.52	35	13.49	41	11.51
Flow out of road 2	15	31.47	17	27.76	18	26.22

[a]DBF is the average distance between flow paths that was calculated by dividing the road length by the number of flow paths.

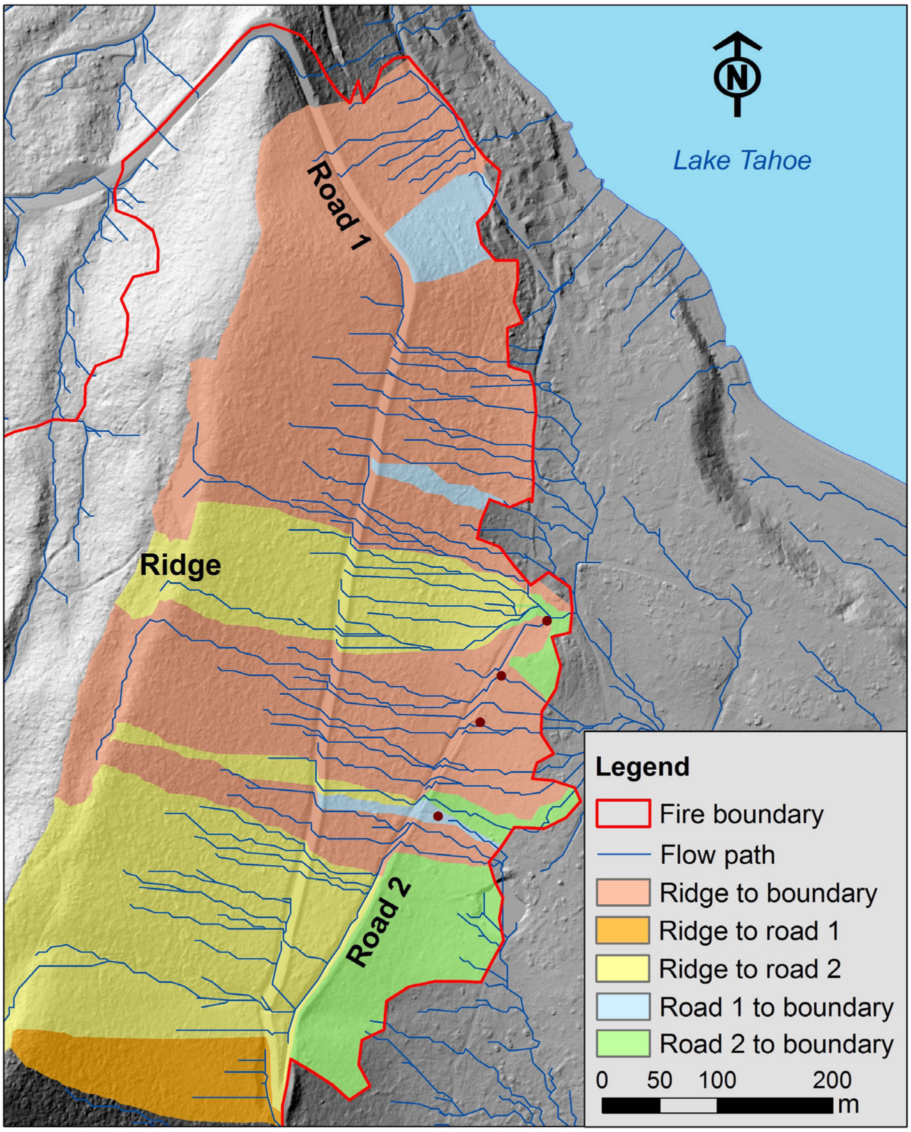

FIGURE 3 Map of the five sub-catchment delineation categories showing the influence of roads on surface hydrology within the 2016 Emerald Fire perimeter (Table 4). The blue lines are ephemeral channels. There were no seasonal or perennial streams within the fire perimeter

with a similar inflow density when CSA was 1000 m^2. In the case of the 200 m^2 CSA, the average distance between outflow paths for road 2 is more than twice the distance than that of the road 1 (Table 3).

The effect of the road segments on sub-catchments as delineated by ArcMap is shown in Figure 3. All sub-catchments in Figure 3 are influenced by roads and can be classified as five types according to the upper and lower extents of the sub-catchments (Table 4; Ridge to lower fire boundary, Ridge to Road 1, Ridge to Road 2, Road 1 to fire boundary and Road 2 to fire boundary). There are 17 sub-catchments that pass over the road segments and finally reach the fire boundary. These hydrologic units account for

TABLE 4 Numbers and areas of road related sub-catchments within the 2016 Emerald Fire perimeter

Type of sub-catchments	Number	Area (ha)	Area ratio (%)
From ridge top to the fire boundary	17	14.85	46.96
From ridge top to road 1	1	1.31	4.15
From ridge top to road 2	10	12.26	38.77
From road 1 to fire boundary	3	0.90	2.84
From road 2 to fire boundary	6	2.30	7.28

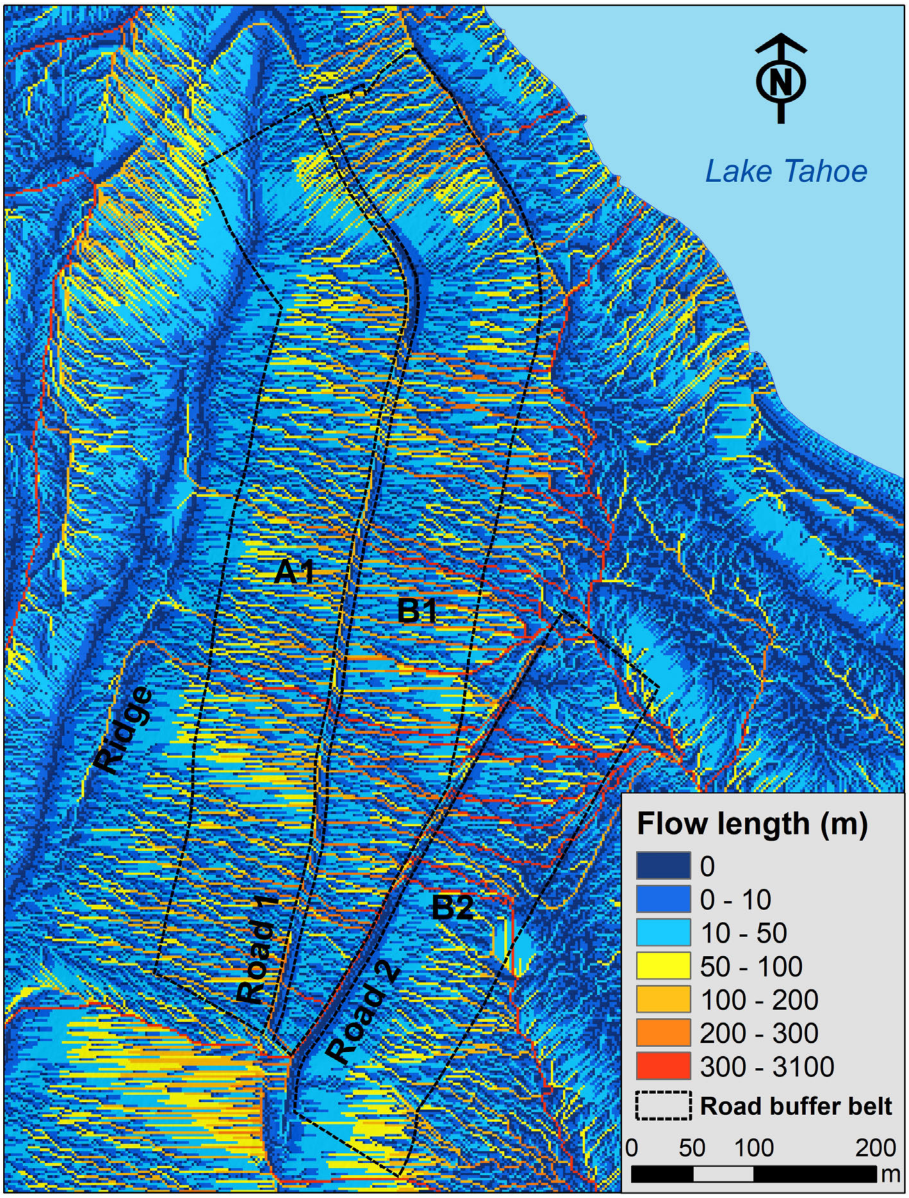

FIGURE 4 The effect of roads on flow path lengths for each 2-m pixel calculated by ArcMap. The outlines for the three belts A1, B1 and B2 that were used to quantify the effect of roads on flow path lengths are delineated (Table 5) for a portion of the 2016 Emerald Fire

47% of the total area. Small channel diversions were predicted when the sub-catchment channels intersected with road segments. 43% of the sub-catchments that started from ridge were intercepted and ended at one of the two road segments with the runoff channelized to another catchment. In addition, 9 new hydrological units were formed downslope of road segments. In spite of being shorter, road 2 with its upslope drain, is more efficient than road 1 in intercepting upstream sub-catchments and generating new ones.

The effect of road segments on surface runoff flow path length is shown in Figure 4. The highly detailed 2-m LiDAR DEM identified a large number of flow initial points (flow length = 0, blue colour) along the ridges and roads. For road 2, which has ditches, many of the upstream flow paths were intercepted. For road 1, which has no

TABLE 5 Average flow length in the different belts (Figure 4) for 2- and 10-m DEMs showing the effect of roads on overland flow path length within the 2016 Emerald Fire

DEM data set	Average flow length (m)		
	A1	B1	B2
2-m LiDAR DEM	32.8	38.1	37.7
10-m USGS DEM	56.1	88.0	131.8

Note: A1 is the area 100 m above Road 1, B1 is the area 100 m below Road 1 and B2 is the area 100 m below Road 2 (Figure 4).

ditches or culverts for most of its length, many upstream flow paths were not intercepted, and flow paths continued over road 1 after an offset (Figures 3 and 4). The flow over road 1 then continued to accumulate length in the downslope direction.

The effect of road segments on flow path was further quantified by comparing individual pixel flow path length values based on the 2-m LiDAR to the flow path length that was determined from a 10-m USGS DEM. Table 5 summarizes the average flow length within three belts: 100 m above road 1 (Belt A1), 100 m below road 1 (Belt B1), and 100 m below road 2 (Belt B2; Figure 4). The flow length layers were overlaid by the belt layers to determine the distributions of flow length values within each belt. The 10-m DEM resulted an increasing average flow length downhill from Belt A1 to Belt B2 from 56 to 132 m (Table 5). The 2-m LiDAR DEM showed little increase of average flow length within the lower Belts B1 and B2, with average path length in all three belts under 40 m, reflecting the fact that road 1 and road 2 interrupted upstream flow paths reducing the flow path lengths below road segments.

3.2 | Soil erosion before and after wildfire

The estimated annual erosion for the prefire condition was less than 0.25 Mg ha^{-1} on nearly 99% of the study area. When burned, erosion risk increased considerably. Figure 5 shows the distribution of sediment delivery by sub-catchment following the fire as estimated by the GeoWEPP Watershed method where the dominant fire severity was estimated for each hillslope polygon. Table 6 shows the distribution of predicted post-fire erosion rates based on the GeoWEPP “Flowpath” method where the erosion rate was estimated for each 2-m pixel as a function of the burn severity, steepness, and location on the flowpath. Post fire predicted erosion rates were greater than 4 Mg ha^{-1} year^{-1} for 77.8% of the pixels (Table 6). After the fire, only 19% of the pixels had estimated erosion rates less than 0.25 Mg ha^{-1}. The high and moderate severity categories account for 46% and 29% respectively of the total study area (Table 2) but accounted for 86.8% of the highest erosion class. 56.3% of the highest eroding pixels (> 4 Mg ha^{-1} year^{-1}) were associated with the high burn severity. The low burn severity and unburned land account for 25% of the total area but only 13.2% of the area with a predicted erosion rates greater than 4 Mg ha^{-1} year^{-1}. The low and unburned areas accounted for 67.8% of the total lowest erosion category (<0.25 Mg ha^{-1} year^{-1}) in the study area.

3.3 | Road segment effect on soil loss prediction

The underlying topography influences the predicted soil erosion rates (Figures 1, 3 and 5). On long hillslopes the high erosion rates were predicted to extended into the unburned area within the fire perimeter (Figures 2 and 5). In some places, road segments intercepted the flow, constraining areas of high sediment yields, particularly below road 2 (Figures 3 and 5). The channel parallel to the upper part of Road 2 is the road ditch that diverted overland flow from above the road to a culvert and sediment basin rather than allowing the surface runoff to spill over the road and increase the likelihood of erosion below the road.

Figure 6 shows the distribution of hillslope soil loss by pixel estimated by running GeoWEPP in the “Flowpath” mode. The erosion rate estimates for the 2-m pixels ranged from areas of deposition to greater than 100 Mg ha^{-1}. The road surfaces showed minimal soil loss and can be distinguished from other areas with the yellow deposition or green zero erosion categories in Figure 6.

Detailed deposition on the surface of road 1 was estimated by running 22 different hillslope profiles that intersected with Road 1 in WEPP Windows. Figure 7 shows the soil loss and deposition distribution along one of these profiles. Figure 7 shows that the erosion rate generally increased as the slope length increased from 0 to 140 m due to runoff accumulation on a relatively uniform gradient. When reaching the road segment, the erosion rate dramatically decreased, and deposition occurred on the road surface section as observed in the three rainy days following the fire. As runoff exited the road and continued flowing downslope, soil loss rate increased sharply within a short distance below road segment. The loss rate reached a maximum value for the profile, and then gradually declined as the increase in accumulated runoff due to increased slope length was offset by a decrease in the hillslope steepness and burn severity (Figure 3). From these runs, the average annual sediment deposition along Road 1 within the fire perimeter was calculated as 40.4 kg m^{-2}, or a sediment deposition depth averaging 4 cm on the surface of Road 1.

The categories of the hydrologic sub-catchments as influenced by roads were shown in Figure 3. Erosion rates were also affected by presence of the roads. Table 7 shows the distribution of onsite erosion determined from the GeoWEPP “Flowpath” analysis (Figure 6) and how it varied with the sub-catchment category (Figure 3) when the sub-catchment image (Figure 3) was overlaid on the erosion image (Figure 6). Table 7 shows that sub-catchments that originated from the ridge resulted in a larger fraction of the high soil loss category (greater than 4 Mg ha^{-1} year^{-1}) than the sub-catchments below roads. The average soil loss rate also showed that sub-catchments below the main ridgeline had the greatest onsite soil loss. Similarly, the sub-catchments below roads showed relatively more deposition and much lower average soil loss rates than those above roads (Figure 6 and Table 7). For sub-catchments below road 2, the average predicted onsite soil loss was negative, indicating that deposition was the dominant process (Table 7).

The GeoWEPP “Flowpath” method that was applied to the hillslopes in the study area considered the burn severity and slope

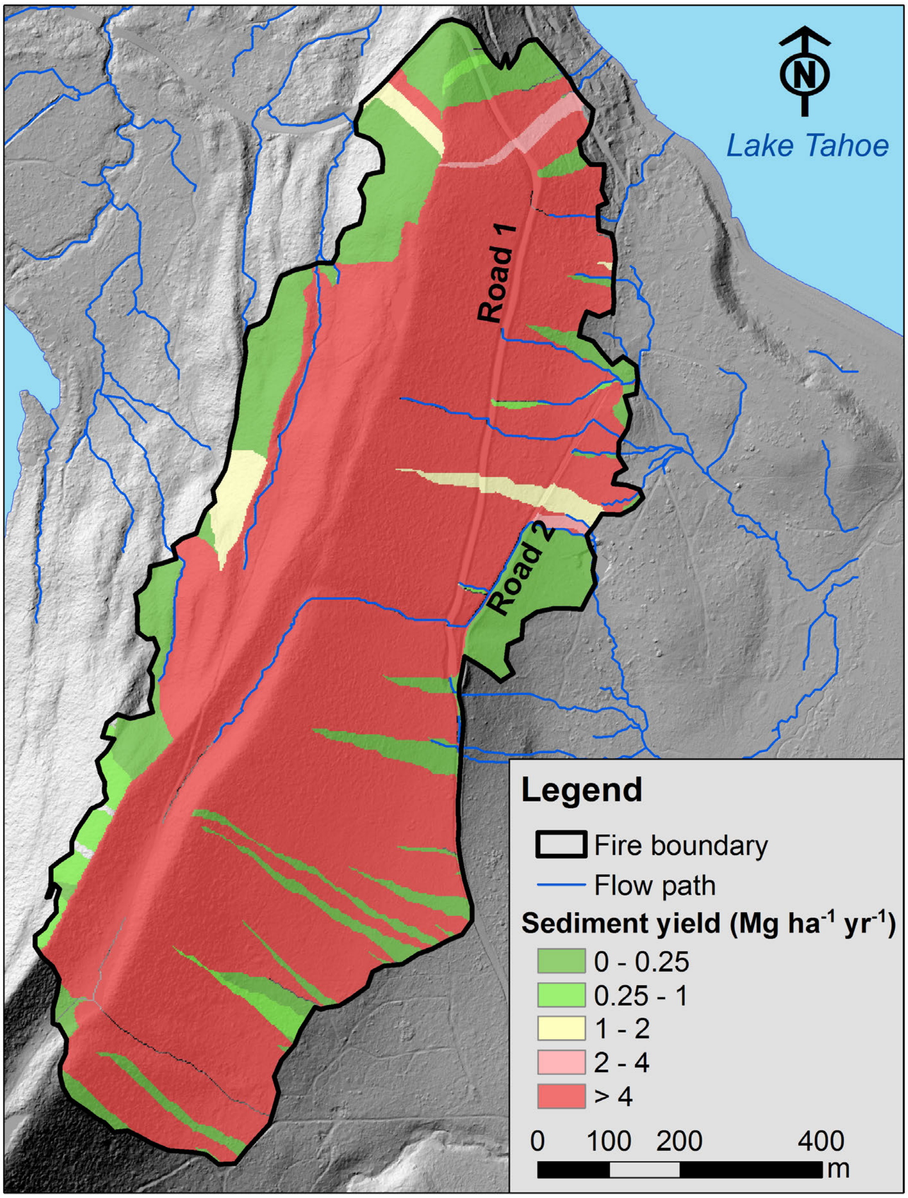

FIGURE 5 Map of estimated sediment yield after the wildfire from each sub-catchment within the 2016 Emerald Fire perimeter showing the influence of the two roads on starting or ending some of the subcatchments. The blue lines are ephemeral channels. There were no seasonal or perennial streams within the fire perimeter

TABLE 6 Distribution of estimated average post-fire erosion rates averaged for all 2-m pixels for each burn severity category following the 2016 Emerald Fire

	Area of different burn severities (ha)[a]				
Erosion rate (Mg ha^{-1} year^{-1})	Unburned	Low	Moderate	High	Total
0–0.25	4.95	3.31	2.92	1.00	12.18
0.25–1	0.66	0.08	0.27	0.27	1.28
1–2	0.43	0.52	0.47	0.26	1.68
2–4	0.10	0.14	0.19	0.07	0.5
>4	3.20	4.03	16.66	30.82	54.71

[a]The total area modelled with GeoWEPP is smaller than the total area in Table 2 because channel areas are not included in GeoWEPP hillslope areas.

steepness and position of each pixel in the watershed to estimate the onsite soil loss or deposition for that pixel. Figures 1 and 2 show that the lower elevations tended to have low to moderate severity burns, whereas the upper elevations tended to have a high severity burn. The spatial distribution of soil erosion (Figure 6) was quantified by a GIS buffer analysis to better understand the interactions among landscape properties, roads, burn severity and estimated soil erosion distribution. The estimated erosion rate was averaged for all pixels within each 10-m-wide belt and plotted with average pixel distance from the ridge or road (Figure 8). Figure 8a shows that the average

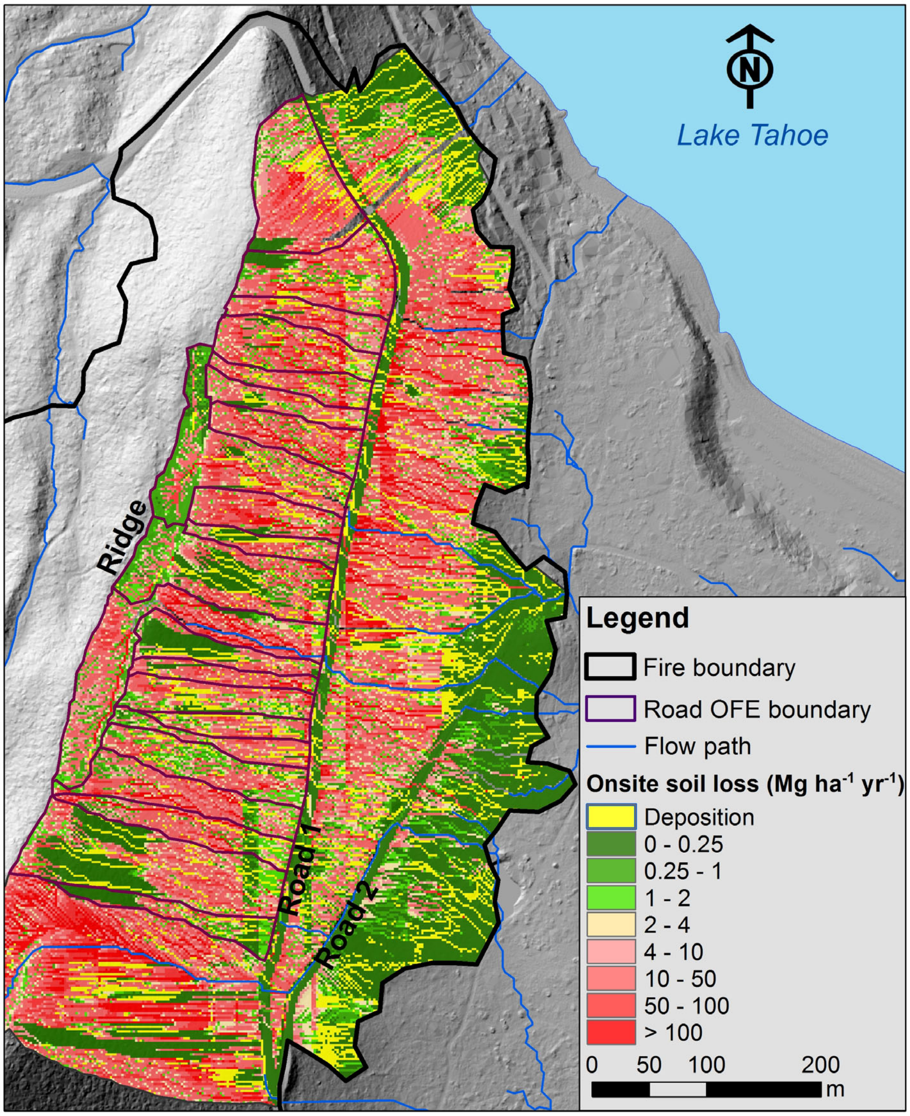

FIGURE 6 Distribution of estimated erosion rates accounting for the burn severity, slope steepness, slope position and road effects for 2-m pixels for the portion of the 2016 Emerald Fire that was influenced by roads. The blue lines are ephemeral channels. There were no seasonal or perennial streams within the fire perimeter

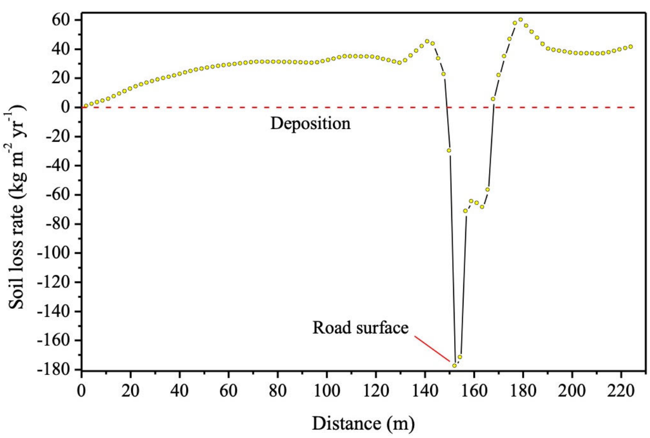

FIGURE 7 Distribution of estimated erosion and deposition (negative soil loss) along an example flowpath that intersects with Road 1 (Figure 3) following the 2016 Emerald Fire

erosion rate below ridge increased exponentially with the downslope distance. On the other hand, the average soil loss rates below both roads 1 and 2 showed logarithmically declining erosion rates with the downslope distance (Figure 8b,c). The average erosion within the first 10-m belt below road 1 is close to that of the last belt below the ridge (Figure 8a,b). Similarly, the average erosion rate within the first belt below road 2 was similar to the last belt below road 1 (Figure 8b,c). Net deposition began to occur about 50 m downslope from road 2 (Figure 8c). This is consistent with the earlier results that measured erosion by sub-catchment category (Table 7) and observations in the field. Note that the average onsite soil loss rate 70 m below road 2 (Figure 8c) showed an exceptionally low value due to the high estimated deposition rates in this belt. This outlier value was not included when developing the regression equation shown in Figure 8c.

3.4 | Comparing modelling results with other model predictions

The initial post-fire erosion analysis (Young, 2016) was carried out by a Forest Service Burned Area Emergency Response (BAER) specialist

TABLE 7 Distributions of estimated average post-fire erosion rates and percent of each rate class for each sub-catchment for 2-m pixels within each sub-catchment category (Figure 3) for the 2016 Emerald Fire

Soil loss rate (Mg ha^{-1} year^{-1})	Ridge to fire boundary		Ridge to R1		Ridge to R2		R1 to boundary		R2 to boundary	
	Area (ha)	Ratio (%)	Area (ha)	Ratio (%)	Area (ha)	Ratio (%)	Area (ha)	Ratio (%)	Area (ha)	Ratio (%)
Deposition	1.48	10.25	0.15	11.39	0.81	7.47	0.15	16.79	0.39	17.87
0–0.25	2.54	17.55	0.55	41.96	0.96	8.84	0.14	15.05	1.21	55.89
0.25–1.0	0.85	5.85	0.03	2.09	0.68	6.31	0.04	4.62	0.15	6.84
1.0–2.0	0.79	5.48	0.04	3.01	0.59	5.44	0.04	4.13	0.09	4.28
2.0–4.0	1.04	7.18	0.05	3.5	0.76	6.96	0.07	7.82	0.14	6.27
>4.0	7.75	53.67	0.5	38.06	7.06	64.98	0.46	51.6	0.19	8.85
Ave. soil loss (Mg ha^{-1} year^{-1})	25.33		28.03		36.38		16.05		−0.06	

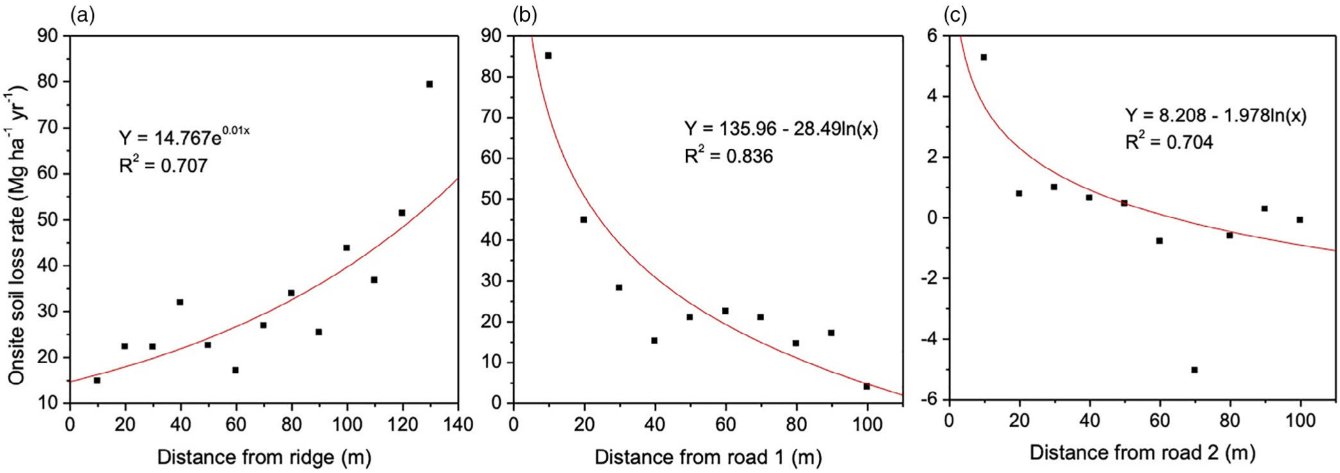

FIGURE 8 The relationship between estimated average erosion rate for every 10-m belt considering each pixel's soil burn severity, slope gradient and downslope distance (a) from the ridgetop, (b) below road 1 and (c) below road 2 for the 2016 Emerald Fire. Negative values reflect sites of deposition in (c)

TABLE 8 Single event runoff, precipitation, and sediment delivery estimated by multiple ERMiT runs for the 2016 Emerald Fire BAER analysis (Young, 2016), and an example of the effectiveness of mitigation practices estimated by ERMiT for a single hillslope (30.7% slope, 60 m long)

	ERMiT return periods		
	2-year event	5-year event	10-year event
Young's (2016) Report			
Runoff (mm)	17.02	29.21	37.34
Precip (mm)	44.20	90.68	35.31[a]
Ave. sediment delivery (Mg ha^{-1})	0.22	6.15	14.76
Max. sediment delivery (Mg ha^{-1})	0.85	29.83	52.51
Sediment production (Mg)	36.18	257.45	538.0
Sediment delivery with mitigation (Mg ha^{-1})			
Average sediment delivery (Mg ha^{-1})	8.37	40.3	53.01
Mulching 1 Mg ha^{-1}	2.02	21.13	32.51
Mulching 2 Mg ha^{-1}	1.84	18.69	22.96
Log erosion barriers, 0.15 m dia, 20 m spacing	0.00	29.58	42.29
Log erosion barriers, 0.15 m dia, 10 m spacing	0.00	23.12	35.83

[a]Runoff is greater than precipitation because of snowmelt during this March runoff event.

using the Erosion Risk Management Tool (ERMiT; Robichaud, Elliot, et al., 2007) to quickly estimate upland erosion following the Emerald Fire (Table 8; Young, 2016). Young (2016) assumed a moderate severity fire and followed recommended methods for applying the ERMiT model (Parsons et al., 2010). He presented the average estimated sediment delivery from 2-, 5- and 10-year events as 0.2, 6. And 15 Mg ha^{-1} respectively (Table 8) having run ERMiT for slopes "parsed into 10% slope classes." The probability of a more severe event was considered unlikely. The three recorded precipitation events that occurred immediately following the wildfire (81, 56, and 114 mm) were similar to the 5 to 10-year return period range of Young's ERMiT predictions for single storms (Table 8). Thus Young's (2016) selection of events was similar to what actually occurred. We estimated spatially averaged total sediment delivery rates for the three rainfall events of 16–25 Mg ha^{-1} for the subcatchments that started at the ridge for the three observed storms (bottom line of Table 7) compared to Young's (2016) estimates of 6 + 15 = 21 Mg ha^{-1} for 5-year and 10-year events (Table 8).

3.5 | Comparison of modelling results to observed sediment delivery

A total of 227 Mg of sediment was removed from the surface of road 1 following the three postfire rainfall events (Vollmer, 2016). The estimated average deposition on road 1 was 40.4 kg m^{-2} (404 Mg ha^{-1} or an average depth of about 4–5 cm) on the road surface (Figures 6 and 7). The length of Road 1 within the fire perimeter is about 790 m, and the width is about 8 m. This means the total estimated deposition is 255 Mg, compared to the 227 Mg of sediment that was removed (Vollmer, 2016). The Windows watershed version for WEPP predicted that 139.6 Mg of sediment needed to be removed from the four sediment basins below road 2 following the October 2016 storms. The amount of sediment removed from these four basins was estimated as 134 m^3 (about 120 Mg; Personal Communication, R. Wigart, Stormwater Coordinator for the Tahoe Basin, Eldorado County, California, 13 December 2016).

4 | DISCUSSION

The objectives of this study were to evaluate the impacts of roads on post-wildfire hydrologic processes, to evaluate the accuracy of post wildfire WEPP predictions and to apply some advanced GIS techniques and WEPP applications to achieve the first two objectives. The results show that these objectives have been met. In addition, the results provide an opportunity to carry out a more rigorous analysis of the interactions among climate, topography, roads, soils and burn severity and how those factors impact hydrologic processes.

4.1 | Interactions among topography and burn severity

The soil burn severity was estimated by remote sensing as described in Parsons et al. (2010) and Robichaud, Lewis, et al. (2007). Robichaud, Lewis, et al. (2007) state that the dNBR method emphasizes the change in vegetation colour from green to black, but also found that the dNBR value is also a reasonable indicator of soil burn severity. Figure 3 shows that the high burn severity was predicted for the steeper, higher elevations on the site. Figure 9 shows the predicted burn severity distribution for three different slope categories. Unburned and lower burn severities are more common on flatter slopes whereas high severity fire was most common on slopes greater than 40%. Andrews (2018) described in detail the Rothermel fire spread model that is common in many current fire spread predictive tools. In the Rothermel model, fire line intensity varies with the square of the tangent of the slope angle, confirming that the steeper elevations in the Emerald Fire would likely experience more severe fire effects. The dominance of lower severity fire at lower elevations, flatter slopes reflects not only the lower slope steepness values, but also the likelihood that soil water contents were higher at lower elevations with concave slopes (Boll et al., 2015) again reducing the fire line intensity (Andrews, 2018).

An alternative method to fire spread models that use the Rothermel equation for predicting soil burn severity is under development. The method uses a statistical technique called "Random Forests" (Breiman, 2001). The method develops a large number of statistical "decision trees" relating burn severity from nearby known fires to landscape properties such as slope, aspect, elevation, curvature, prefire fuel properties and climate variables. From the decisions trees that are developed, soil burn severity can then be estimated for nearby unburned areas. This technique was applied to the Lew et al. (2020) watershed analysis of the western slopes of the Tahoe Basin using the 0.71-km^2 Emerald Fire, the 2007 Angora Fire that burned 12.5 km^2 located 9 km south of the Emerald Fire within the Tahoe Basin, and the large 2014 King Fire that burned 395 km^2 47 km southwest of the Emerald Fire. Two of the variables found to be statistically important for predicting burn severity when all three

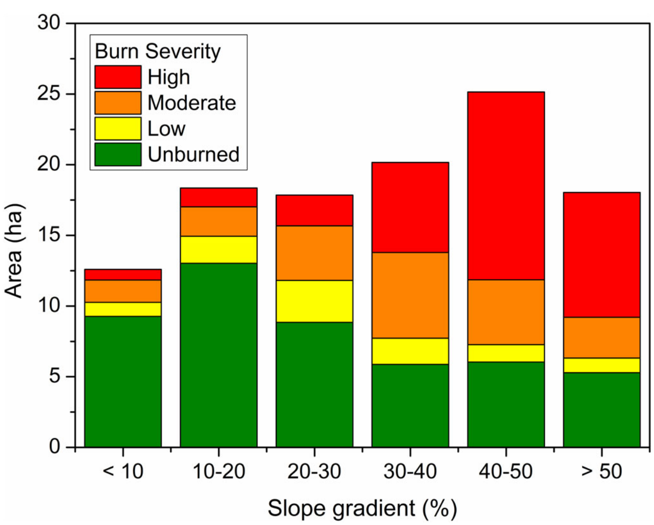

FIGURE 9 Distribution of burn severity as determined by the dNBR method for different slope gradients for the 2016 Emerald Fire

fires were combined for the analysis were elevation and slope steepness, with more severe fires on steeper slopes at higher elevations (M. Dobre, personal communication, February 2021), confirming that the burn severity distribution for the Emerald Fire as determined by our dNBR analysis was similar to the two larger nearby fires.

Elliot et al. (2016) reported on several studies that used fire line intensity as a surrogate for soil burn severity when linking Rothermel fire spread models to erosion models, one of the studies only 30 km south of the Emerald Fire site. The dNBR results of this study confirm the reasonableness of linking a simulated wildfire to an erosion model for proactive fuel management planning (Elliot et al., 2016; Srivastava et al., 2018). In the Srivastava et al. (2018) study linking a burn severity model to an erosion model, they found results similar to Figure 9 showing higher severity fires predicted for steeper slopes and they linked the increased fire severity combined with increased slope gradients to higher erosion rates. Table 6 shows that in this study, the areas with high severity fire had the majority of estimated high erosion rates.

4.2 | Estimated erosion in "unburned" areas

The fire perimeter was defined by the Forest Service from satellite imagery. Within that perimeter, 9.34 ha were categorized as "unburned" in our burned area reflectance category (BARC) analysis (Table 2; Parsons et al., 2010). A post-fire site visit by the authors confirmed that there had been an under burn in much of the lower elevation of the fire, but the canopy was relatively unburned, hence the "unburned" classification from the BARC map analysis that was based on satellite imagery.

The prefire erosion rate was estimated to be less than 0.25 Mg ha^{-1} $year^{-1}$. However, a third of the unburned areas post fire had estimated erosion rates greater than 4 Mg $ha^{-1}year^{-1}$ (Table 6). The unburned patches were at the bottom of most of the slopes (Figure 2) in the "Road 2 to boundary" category (Figure 3; Table 7). The estimated high erosion in the unburned areas was likely due to presence of a high severity burn upslope from some of the unburned patches generating high runoff rates with eroding rills that extended well into the unburned patches (Figures 2 and 3), resulting in the elevated erosion rates on those unburned patches within the fire perimeter. Had we extended the modelling beyond the fire perimeter; we would have likely identified additional unburned areas with elevated erosion rates.

4.3 | Climate selection

The elevation of the Echo Peak SnoTel station that provided the climate information for this study is 2338 m (NRCS, 2020). The elevation of the study site is 1900 to 2100 m. The onsite storm depths that caused the observed erosion may have been less than the values we used that were recorded at the higher elevation SnoTel site because of orographic effects. An online WEPP climate file builder (https://forest.moscowfsl.wsu.edu/cgi-bin/fswepp/rc/) was accessed to evaluate differences in precipitation and temperatures between the study site and the SnoTel station. This online climate file builder uses the 4-km resolution PRISM climate database (Scheele et al., 2001) to incorporate differences in climate due to site elevation and other factors. The average annual precipitation for the Echo Peak SnoTel site was 1552 mm. The PRISM average annual elevation for the grid containing the SnoTel station was 1016 mm, and for the 4-km grid cell for the Emerald Fire site was 640 mm. The average October precipitation amounts for the SnoTel site, the SnoTel PRISM grid, and the study PRISM grid were 79, 53 and 35 mm, respectively. Since this study used the SnoTel data for both the prefire and the post fire analysis, it is likely that the predicted erosion rates are overestimated. However, Vollmer (2016) reported that local observations near the fire had reported precipitation depths ranging from 127 to 178 mm for the 3 days following the fire, compared to 251 m at the SnoTel site, suggesting that the long term average differences in the PRISM database are likely greater than the spatial differences for large events. Vollmer (2016) reported that the Lake level increased by 84 mm following the 3 days of rain, increasing the volume of water in the lake by 42 million m^3, reflecting the large aerial impact of this event. For one observed large historic flood event in the Tahoe Basin in 1997, Brooks et al. (2016) found that a lower elevation weather station resulted in better modelling performance than a higher elevation station nearer the center of the watershed, and they stated that "the hydrologic response of a watershed to large intense storms is highly sensitive to how well the storm pattern is represented in the input data". This suggests for big events, like those in October 2016, could have been more or less intense on the study site than what was measured at the nearest SnoTel station, depending on the storm pattern.

4.4 | Selection of soil erodibility properties

Objective 2 was, "From the observed depositions, is it possible to evaluate the accuracy of the WEPP post fire runoff and erosion tools?". No calibration of the WEPP model was carried out as part of this study in order to meet this objective. The soil erodibility properties presented in Table 1 were downloaded from the Miller et al. (2015) online database for this fire and from Elliot and Hall (2010) for the road properties; no recalibration was done. This is the same database that is used by the USDA Forest Service and other land managers for evaluating post wildfire risks with GeoWEPP or QWEPP. The Miller et al. (2015) and Elliot and Hall (2010) WEPP forest soil erodibility databases are similar and the database for modelling the other watersheds on the West Shore of the Tahoe Basin was developed from them (Lew et al., 2020). The results of this study suggests that the WEPP technology does predict reasonable post fire sediment delivery rates using these databases.

The effective hydraulic conductivity values presented in Table 1 are for the Green-Ampt equation incorporated into the WEPP model. Nearing et al. (1996) state, "The Green-Ampt effective hydraulic conductivity parameter K_e is approximately equal to one-half the saturated hydraulic conductivity of the soil, K_s". The values for K_e in the Miller et al. (2015) database are based on rainfall simulation studies such as reported by Larson-Nash et al. (2018), Pierson et al. (2008) and Robichaud, Wagenbrenner et al. (2016). The post-wildfire steady state infiltration rates reported by Larson-Nash et al. (2018) on a sandy loam soil were 15 mm h^{-1} on 20%-slopes and 40 mm h^{-1} on 60%-slopes on the burned plots and 65 mm h^{-1} and 40 mm^{-1} on unburned plots on 20% slopes and 60% slopes, respectively. The Pierson et al. (2008) study reported results from three different rangeland fires, stating that post-fire final infiltration rates were 27.6 to 57.6 mm h^{-1}, compared to control plots with final rates of 56.4 to 72.3 mm h^{-1}. and the Robichaud, Wagenbrenner et al. (2016) were 20–40 mm h^{-1}, The conductivity values from these studies were generally reduced about 40% in line with the findings of Nearing et al. (1996) for the Elliot and Hall (2010) soil properties database that were used in this study.

The effective hydraulic conductivity values measured by rainfall were subsequently validated or modified with forest watershed validation studies such as post fire modelling by Dun et al. (2009) who calibrated a value of 90 mm h^{-1} for a 9-ha watershed with a low severity fire and Quinn (2018) who assumed effective hydraulic conductivity values for unburned, low, moderate and high severity of 100-, 10-, 1.0- and 0.1-mm h^{-1} for a 117-ha watershed with mixed burn severities. Dun et al. (2009) had a Nash and Sutcliffe (1970) efficiency of 0.45 for daily runoff values in their study, and Quinn (2018) reported a Nash-Sutcliffe efficiency of 0.5 for daily runoff estimates. Srivastava et al. (2013) calibrated K_e values for forests of 50.4 mm h^{-1} on a 5.5-ha forested watershed with a silt loam soil in Northern Idaho, USA. In Srivastava et al. (2017) values for K_e were calibrated to be 102 and 330 mm h^{-1} on 105-km^2 forested sandy loam and loamy sand soils in Western Washington, USA. The Nash-Sutcliff efficiency of daily runoff for Srivastava et al. (2013,2017) studies were 0.67 and 0.75 respectively. All the studies achieved a reasonable Nash-Sutcliffe efficiency value, and all studies noted in their discussion that runoff was dominated by shallow lateral flow or base flow, and not surface runoff. In the Dun et al. (2009) study no surface runoff was observed, nor was there any evidence of surface runoff in the Srivastava et al. (2013) study. The calibrated and validated effective conductivity values from the watershed studies confirm the rainfall simulation findings, that effective conductivity values are much lower following wildfire, and that the Green-Ampt effective conductivity values are lower than observed saturated hydraulic conductivity. These studies show a wide range of hydraulic conductivity values, with lower values following wildfire compared to unburned conditions, and that the values in Table 1 are reasonable.

The findings from the WEPP-related studies can be compared to studies by others focusing on hydraulic conductivity or infiltration rates following wildfire. Moody et al. (2016) reported on a study directly linking saturated hydraulic conductivity values to dNBR values for a sandy loam soil. They took soil cores from sites with a range of dNBR values following a wildfire in Colorado, USA and in a laboratory setting, measured the infiltration rate with a "mini-disk infiltrometer". They used the observed infiltration rates to estimate saturated hydraulic conductivity, and then developed a relationship between dNBR and saturated hydraulic conductivity. From the observed mini disk infiltration rates, calculated saturated conductivity values for dNBR values of 124, 227, 420, 672, 753 and 886 were 8.1–791, −0.2 – 23 486, 22–555, 22–285, 9–374 and −13–50 mm h^{-1}. They deleted the negative values and some of the outliers in the data set, calculated the geometric mean for each dNBR category and developed the relationship:

$$K_{fs} = 147 \text{ for } 124 \le \text{dNBR} < 420) \tag{1a}$$

and

$$K_{fs} = 2360\, e^{-0.0056\,\text{dNBR}} \text{ for } 420 \le \text{dNBR} \le 886 \tag{1b}$$

where K_{fs} is the "field saturated hydraulic conductivity". Assuming that the Green-Ampt effective conductivity is about 40% of the saturated hydraulic conductivity, Equation (1) would result in estimated hydraulic conductivity values of 88.2 mm h^{-1} for unburned and low severity categories, 35. mm h^{-1} for moderate severity, and less than 35 mm h^{-1} for high severity. These values are somewhat greater to those used for this study as presented in Table 1. The constant value for unburned and low severity fires that Moody et al. (2016) proposed Equation (1a) was based on the NRCS soil survey for the study location and was much smaller than the values that would have estimated with Equation (1b). Moody et al. (2016) also reported that Equation (1b) predicted saturated hydraulic conductivity values about twice the values measured by the same procedure for wildfires elsewhere in Colorado and California, USA, and Victoria, Australia. Larson-Nash et al. (2018) compared infiltration rates measured with the same type of minidisk infiltrometer as used by Moody et al. (2016) to rates measured with rainfall simulation in the field and found a significant statistical correlation between the two methods. The Moody et al. (2016) findings also highlighted the high variability associated with post-fire soils, with the range of observed infiltration rates resulting in calculated values of saturated conductivity ranging from a negative value to greater than 200 000 mm h^{-1}.

Using an onsite double ring infiltrometer method, Cole et al. (2020) reported a post-fire field saturated hydraulic conductivity measurement of 455 ± 267 mm hr^{-1}, confirming the large variability associated with measuring this property, as well as the effect of measurement methodology on the value. Robichaud et al. (2020) determined that infiltration rates on a simulated rill experiment immediately following a wildfire were 230 mm hr^{-1}, similar to Cole et al. (2020), and were greater than 2000 mm hr^{-1} on nearby unburned sites. In both Cole et al. (2020) and Robichaud et al. (2020) studies the positive head due to the infiltrometer depth or rill depth would have caused a greater infiltration rate than would occur from rainfall or snowmelt when there would be a minimal head from water ponded on a natural landscape. The large variability that is common in the post-fire landscape and was one of the reasons why the ERMiT interface was developed, to incorporate the variability of post-fire soils into erosion prediction (Robichaud, Elliot, et al., 2007; Robichaud, Elliot, et al., 2016). Such variability also underscores the stated accuracy of WEPP predictions in forests of the true value that is likely to be within plus or minus 50% of the mean (Elliot et al., 2000).

Following a wildfire, two of the observations carried out on the burned area with respect to soils are ground cover and water repellency (Parsons et al., 2010; Robichaud et al., 2020). In addition, Parsons et al. (2010) recommend that soil surveys be consulted to determine the soil texture class. In Elliot and Hall (2010) database, if the soil is water repellent, it is considered “high severity” and if it is not water repellent, the soil is considered “low severity”. The difference then, between “low severity” and “moderate severity” is the ground cover. In the context of the WEPP model, ground cover includes vegetation, organic material and rocks greater than 2 mm diameter (Elliot & Hall, 2010).

One of the ongoing challenges in the post fire management is that the dNBR mapping is a measure of vegetation burn severity (Robichaud, Lewis, et al., 2007). Parsons et al. (2010) recommend that a ground survey be carried out to adjust the vegetation category to better describe the soil severity category. In this study, the Tahoe soils tend to be naturally water repellent, so assuming a “high severity” soil condition is reasonable where the dNBR suggests high severity. With the large amount of ground cover observed after the fire in the moderate and low severity areas, the areas classified as “moderate” and “low severity” from the dNBR results support linking a “low severity” soil to these categories. The ground cover values used in Table 1 were intentionally defined at the lower end of the range of commonly observed values to make sure that erosion results were not underestimated.

The Miller et al. (2015) soil files combine the WEPP erodibility values (Table 1) with the soil textures, rock content and organic matter for up to 10 layers or 2-m depth of soil profile from the SSURGO or STATSGO soil databases. Because of the inherent variability of soil erodibility properties, and the limited number of field studies on post-wildfire soil erodibility, the WEPP soil erodibility database is limited to only four textures: sandy loam, silt loam, clay loam, and loam. There is a need to find the resources to expand this database through additional rainfall (Pierson et al., 2008) and runoff (Wagenbrenner et al., 2016) simulation studies, as well as post wildfire small watershed calibration and validation analysis (Quinn, 2018; Srivastava et al., 2013, 2020). However, we have found that the presence of water repellency (“high severity” vs. “low severity”), the post-wildfire groundcover, and the profile depth make much greater differences on estimating soil erosion with WEPP than do soil properties associated with the textural classification.

With hundreds of inputs needed for a given WEPP run, there is always a risk for equifinality in the WEPP predictions when it is possible to get the right prediction but for the wrong reasons. For example, if runoff is overpredicted and erodibility under predicted, sediment delivery may still be correct. This study only had observed sediment deposition to compare with the predicted values, as there was no measurement of runoff. The above discussion about WEPP's hydrologic performance shows that others have found the WEPP hydrology is reasonable (Dun et al., 2009; Quinn, 2018; Srivastava et al., 2013,2017), as do the results comparing observed stream flows to estimated stream flows for the unburned gaged watersheds within the Tahoe Basin (Lew et al., 2020). The stated accuracy that erosion prediction model can be no better than plus or minus 50% of the mean Elliot et al. (2000) applies to this study, and indeed to any erosion prediction, Sources of error in model inputs and internal assumptions and calculations are common to all erosion prediction tools.

4.5 | Downslope distance versus flowpath length

Figure 8 showed the average pixel erosion rate as a function of distance below the ridgetop, road 1 and road 2. The curves reflected not only flow length, but also the decline in slope steepness and reduction in burn severity with downslope distance. Maximum distances exceeded 100 m for all three categories. Figure 4 shows that hillslope flow path lengths, however, seldom exceed 100 m unless the flow has been channelized. To better understand the effects of flow path length and steepness, and not just landscape position on soil erosion, the flow erosion rates for each 10-m belt were plotted against flow path length (Figure 4) and flow path gradient (Figure 10). For the belts below the ridgetop, Figure 10a is similar to Figure 8, with erosion rate increasing exponentially with distance on the relatively uniform topography and burn severity (Figure 2). The combined effects of a declining slope gradient and lessening of burn severity result in a much steeper reduction in erosion rate with distance below Road 1 than suggested in Figure 8. Also, because Road 1 was outsloped allowing flowpaths to continue over the road, the flow paths were longer for this category. Road 2 was insloped with an upstream ditch (Figures 2, 3 and 5), resulting in shorter flow paths than observed below Road 1. The lower gradients and lower severity fire on the belts below Road 2 resulted in the lowest estimate erosion rates even though the flow path lengths were similar to the other categories. Figure 10b confirms the lower slope gradients below Road 2. The decline in erosion with increasing slope gradient in the “From the ridgetop” belt is noteworthy. What the results suggest is that steeper slopes, tend to be shorter, and that the combined interaction of slope length and steepness leads to an overall decline in erosion with steepness. This can be ascertained by noting that the highest average erosion rate for this belt has one of the lowest gradients (Figure 10b), but the longest flow length (Figure 10a), whereas the lowest erosion rate in this belt has the lowest flow length, but one of the highest slope gradients. Another possible cause for decreased erosion on steeper slopes is that steeper slopes may have higher subsurface lateral flow rates (Boll et al., 2015), resulting in less surface runoff and erosion, but increased surface flow rates as slope gradients moderate, resulting in more surface runoff, and increased risk of erosion.

4.6 | Road segment effect on surface flow patterns and soil loss

This is a relatively small fire, and therefore the ability to evaluate all of the complex interactions that may occur between roads and a post

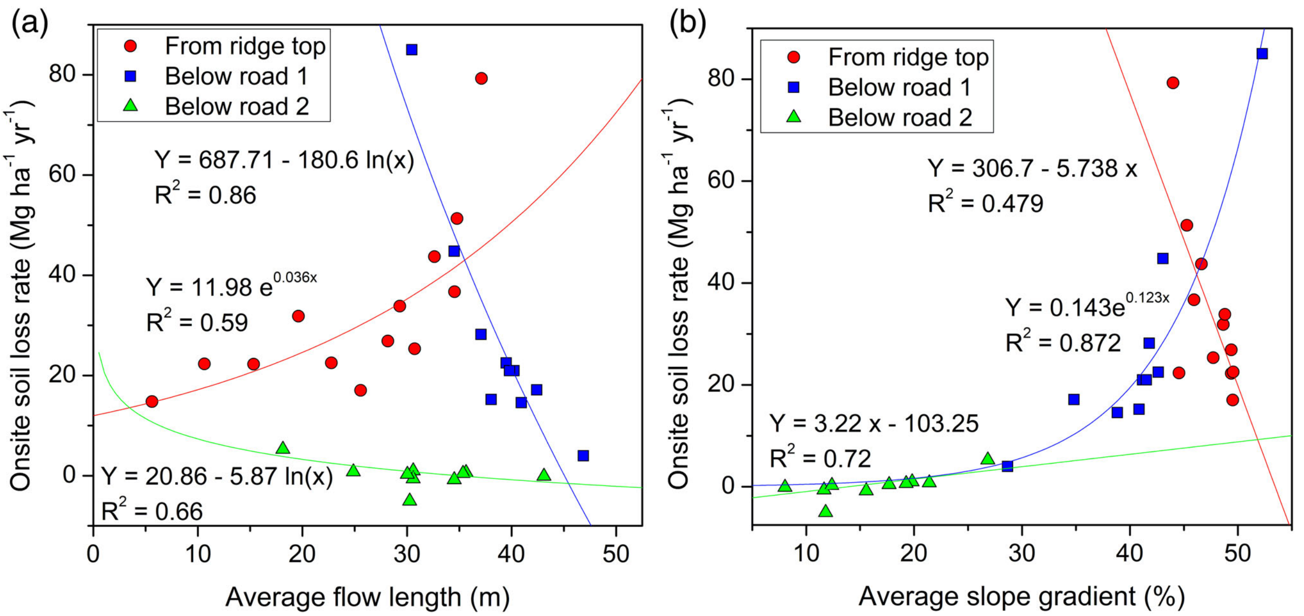

FIGURE 10 The average pixel soil loss rate versus the average pixel flow path length (a) and average pixel slope gradient (b) for each 10-m wide belt below the ridge, below road 1 and below road 2, assuming the burn severity distribution in Figure 2 and the slope and position of each pixel following the 2016 Emerald Fire

fire landscape is limited. The study did, however, contain both paved and gravelled roads, and insloping and outsloping road designs. It also had roads greater and less than the 5% inflection point that Sosa-Pérez and MacDonald (2017) had identified as the point where sediment deposition decreased, and detachment increased on road surfaces.

The ArcMap flow path analyses showed that roads reduced the number of flow paths (Table 3). Road 2 showed a greater reduction in flow paths than road 1. This is likely due to the ditch on the uphill side of the upper part road (Figures 3 and 5), intersecting more flow paths and diverting more dispersed runoff to fewer locations. The outsloping design of road 1 did not cause as great a reduction in flow paths. The distance between flow paths in Table 3 varied from 7.4 to 31.47 m, depending on the CSA and location. For the WEPP watershed modelling, a CSA of 5000 m^2 was specified, so the distance between flow paths will greater than 20 m (Table 3). WEPP assumes a default rill spacing of 1 m, and this was not altered for the analysis, so the CSA value is unlikely to impact the rill erosion estimate.

The average flow path lengths with and without the presence of roads was summarized in Table 5. The shorter flow path lengths due to the presence of the roads will likely result in a lower rill erosion rate (Finkner et al., 1989; Miller et al., 2011). A 10-m DEM was used to mask the road effects that were predicted with the 2-m LiDAR DEM. A coarser DEM will also contribute to the longer flow path length calculation in a GIS analysis even if there are no roads in the catchment (J. X. Zhang et al., 2009). J. X. Zhang et al. (2009) compared a Geo-WEPP analysis with a 4-m resolution LIDAR to the 10-m resolution USGS DEM on 2 small forested and roadless watersheds in Idaho, USA, and found that the average hillslope length increased from 188 to 209 m on one watershed, and 190 to 213 m on the other with the coarser DEM. J. X. Zhang et al. (2009) did not analyze flow individual flow path lengths in their study, but the longer hillslope lengths for the coarser DEM in their study would likely contain longer flow path lengths.

Generally, the net effect of road networks in a forest is to increase basin-wide sediment production (Brooks et al., 2006; Grace, 2017; Soulis et al., 2014; Wemple et al., 2001). However, sediment deposition is also likely where sediment-laden overland runoff reaches low gradient road surfaces, (Finkner et al., 1989; Gucinski et al., 2001; MacDonald & Coe, 2008). In post-fire conditions, Sosa-Pérez and MacDonald (2017) found that sediment deposits were much more likely on roads with gradients less than or equal to 5%. In this study, Road 1, the highway, had a gradient of about 4%, and had more than 200 Mg of observed deposition, or about 360 Mg ha^{-1}. Road 2, a gravelled road, had a gradient of 7%, and little deposition was observed in the road drains or surface during a site visit. The results in Tables 3 and 5, and Figure 4 show that road segments intercepted upstream runoff; and in Figures 6 and 7, were sites of sediment deposition.

Two processes account for the high onsite soil loss rate within the 10 m buffer belt below Roads 1 and 2 (Figures 8b,c and 10a) and the sharp erosion increase after leaving the road in Figure 7. First, with the large amount of post-fire sediment deposition along road surfaces, the increased flow below roads has a relatively low sediment concentration and therefore can detach more soil particles (Finkner et al., 1989). Secondly, Road 1 has over-steepened fillslopes (Figure 10b), because the excavated material upslope of the road centerline is placed on the downhill side of the centerline with a 50% (26°) slope or greater on steep hillsides. Further downhill, the slope decreases as does the predicted erosion rate, until ultimately, deposition begins to occur (Figures 7, 8b,c and 10a). Miller et al. (2011) carried out a sensitivity analysis demonstrating that WEPP estimates a logarithmic increase in erosion with slope gradients up to 120% (50°), and thus is able to consider the range of observed gradients in this study.

Figures 3–6 all show different ways of visualizing how a road can alter the boundary of sub-catchments and hydrological units on a post-fire landscape. Table 4 and Figure 3 show that a road segment can act as a boundary between sub-catchments, and in some cases, forming new sub-catchments below a road (Figure 3). The new sub-catchments below roads tend to have shorter flow paths, and hence, are at less risk to concentrated flow erosion (Table 7). On the other hand, the flow length accumulations for some flow paths passing over the roads in Figures 3 and 4 show that road segments can also function as flow diverters, transporting sediment from one sub-catchment to a nearby sub-catchment in some cases (Gucinski et al., 2001). Road 2 is a good example of flow diversion as the upper part of the road has been identified as forming an adjacent channel in Figures 3 and 5, diverting the runoff and sediment yield to an adjacent sub-catchment (Gucinski et al., 2001).

4.7 | The importance of road design

Our results show the importance of the road drainage system in a post-fire watershed in altering surface hydrologic and soil loss processes. A field survey confirmed the LiDAR topography with road 1 is relatively flat and lacking culverts or an inside drainage ditch within the eastern part of the burnt area. Much of the upslope runoff either followed or crossed over the road surface (Figure 3), depositing sediment as it passed (Vollmer, 2016). Conversely, there were several ditches defined by the LiDAR DEM and verified by our field visit along road 2 (Figures 3 and 5). Road-intercepted runoff was channelled along the road 2 ditches to culverts and downhill sediment basins rather than flooding over the road surface. Therefore, the land surface below road 2 was not impacted by upslope runoff and the erosion risk was limited to channels (Figure 5). The upslope armoured ditches and regularly spaced culverts on road 2 demonstrate the potential for road networks to reduce erosion risks in forests following wildfire.

This study found that following a wildfire, roads may be sites of flow diversion, and sediment deposition if the gradient was low. This finding was in keeping with the findings of Sosa-Pérez and MacDonald (2017) who noted that in runoff events following a wildfire in Colorado, USA, that upland sediment upon reaching road gradients under about 5% tended to deposit, whereas intercepted runoff on native-surfaced roads with gradients greater than 5% tended to cause erosion. Sosa-Pérez and MacDonald (2017) also used flow path modelling to determine that road segments could divert hillslope and road surface runoff to a single drainage point. From this perspective, a road can act as a hydrologic barrier and reduce sediment yield in a fire disturbed forest on lower gradient roads (Gucinski et al., 2001; Sosa-Pérez & MacDonald, 2017). The ability of roads to manage overland flow means that there is a potential on higher gradient roads to incorporate conservation measures such as armoured ditches and sediment basins into road drainage designs. An example of these measures is the use of sediment basins installed below culverts on road 2 making it unnecessary to treat the whole area below road 2 to limit erosion (Figure 5).

The sediment basins were located near the lower boundary of the fire perimeter and on lower slopes (Figure 1). Any overflow from the basins was concentrated, and not contributing to the erosion of the hillslopes adjacent to those flow paths (Figure 4) In reality, the overflow may have dispersed on the low gradient hillslopes below the basins, and caused some additional erosion risk on those low gradient slopes, but our current modelling capabilities did not allow us to consider this possibility (Elliot & Tysdal, 1999).

4.8 | Comparison to other erosion estimates

The three observed post-fire storms were similar in magnitude to Young's (2016) ERMiT predictions for one 2-year event (0.22 Mg ha^{-1}), one 5-year event (6.15 Mg ha^{-1}) and one 10-y event (14.76 Mg ha^{-1}, Table 8) for a total of about 21 Mg ha^{-1} compared to the predictions of this study for the ridge to boundary average prediction of 25.33 Mg ha^{-1} for the three storms (Table 7). Young's rapidly completed predictions, with a stated accuracy of plus or minus 50%, are similar to our more detailed analyses, confirming that the coarse-scale ERMiT predictions are reasonable for rapid post wildfire erosion analysis within the Tahoe Basin. In studies of the performance of ERMiT outside of the Tahoe Basin, Robichaud, Elliot, et al. (2016) concluded that ERMiT "model validation results suggest reasonable estimates of probabilistic post-fire hillslope sediment delivery when compared with observations from eight field sites". The current BAER erosion prediction technologies as exemplified by Young (2016), however, did not consider the effects of roads in his analyses, which we have shown can be significant (Table 7). For comparison, in an erosion study on the 2016 Valley Fire, located 260 km NW of the Emerald Fire, Cole et al. (2020) reported an erosion rate of 13.3 Mg ha^{-1} year^{-1} on slopes of 22% to 31% steepness with a sandy loam soil. They did not report any severe storms like those that immediately followed the Emerald Fire.

The comparisons of predicted sediment deposition rates to observed deposition on Road 1 (255 vs. 227 Mg) and in Road 2 sediment basins (140 vs. 120 Mg) was encouraging. The overpredictions for both values may have been due in part to the climate that was used, as previously discussed. More rigorous comparisons between sediment delivery observations and model estimates are necessary over a wide range of post fire conditions to fully evaluate the WEPP model's performance for such complex modelling scenarios. To our knowledge, this is the only study that has evaluated the performance of sediment basin modelling with WEPP compared to field observations. Such post-fire comparisons, however, are not easily achieved as erosion monitoring equipment is seldom in place when a fire occurs, and by the time such equipment could be installed within a year following the fire, erosion risks have significantly declined (Larson-Nash et al., 2018; Robichaud, Elliot, et al., 2007; Robichaud, Elliot, et al., 2016; Robichaud et al., 2020).

4.9 | Estimated impacts of erosion mitigation

The Emerald Fire was stopped by 3 days of rainfall, so there was no opportunity to instal any mitigation measures, such as log erosion barriers oriented on the contour or mulching after the fire but before these events. The GeoWEPP technology is not able to model any finer resolution than a 2-m pixel, so the effectiveness of log erosion barriers cannot be evaluated with this tool. GeoWEPP has been used to model the effectiveness of mulching in numerous fires in recent years but such an analysis was beyond the scope of this study. Young's (2016) analysis, however with the ERMiT tool did provide an opportunity to evaluate the effectiveness of erosion mitigation. To give an example of the benefits of mitigation, the ERMiT model was run for a 60-m long hillslope with steepness values of 30.7%, 30.7% and 21.8% along the slope, with a moderate severity fire, similar to the conditions that Young (2016) had used for preparing his report. Table 8 shows that mulching reduces the estimated sediment delivery about 50%, and contoured logs by 10–12 Mg ha^{-1}, depending on the log diameter and spacing. Since the fire, straw wattles have been installed on the upper slopes, and ground cover has increased due to the burned trees shedding needles that were not burned, reducing the risk of additional erosion on the site.

4.10 | Implications for post-fire management

In the absence of wildfire, upslope runoff and sediment generation are minimal from the mature forests in the study area (Brooks et al., 2016; Lew et al., 2020; Nevada Division of Environmental Protection, 2011). When forests are burned as in this study, surface runoff and soil erosion are greatly increased. From the limited sedimentation observations in this study, when combined with other validation studies, it appears that the WEPP and ERMiT technologies can provide reasonable estimates of post fire erosion and sedimentation rates in the Tahoe Basin. This suggests that these tools can be utilized for post fire response such as Young (2016) and to support watershed planning activities such as Lew et al. (2020).

Road segments can intercept post fire flow paths for surface runoff, especially when flow path networks are dense (Table 3). This implies that roads will be relatively more efficient in altering surface flow pattern under the post-fire conditions that generate more flow paths, as may occur with larger or more intense storms as was the case in this study, or on soils with lower hydraulic conductivity. The lower conductivity could also be due to inherent soil properties or water repellency as is common in the Tahoe Basin when undisturbed soils are dry (Johnson et al., 2009) or following a wildfire (DeBano, 2000; Doerr et al., 2000; Larson-Nash et al., 2018; Moody et al., 2013; Sheridan et al., 2007). By intercepting upstream runoff, road segments may prevent sediment transport to downstream channels.

Roads can intercept the high sediment loads that result from surface erosion from upslope burned areas as observed with Road 1. After a fire, sediment and other debris can accumulate and block ditches and culverts, leading to road damage and failures that compound the erosion (Foltz et al., 2009). Sediment basins, channel energy dissipation structures and in-channel grade control structures (Napper, 2006; Robichaud et al., 2019) may be beneficial to control erosion on channels below roads and to reduce the risk of gully initiation (Zhang et al., 2019).

The advanced watershed planning tools such as flow path analysis, belt analysis and multiple DEM resolutions down to 2 m in ArcMap, GeoWEPP, and WEPP Windows are useful for evaluating complex topographical and land cover interactions. The methods described in this study can be used in other disturbed watersheds where water quality management is critical, not only after fire, but after other disturbances such as road network management (Elliot, Miller, et al., 2018), construction (Laflen et al., 2001), mine reclamation (Liu et al., 2015) or terracing (Flanagan & Livingston, 1995).

4.11 | Future research needs

The Emerald Fire was small, but it is clear from the results of this study, that the two roads within the fire perimeter likely decreased the upland erosion rate and off-site sediment delivery. There is a need for studies that measure sediment from both roads and disturbed landscapes to gain further information to assist in improving road design and management, and watershed modelling. To complete this study, we employed some novel GIS and WEPP applications that would likely require more time to carry out following a wildfire than was available (Miller et al., 2016), and may be beyond the expertise of post-fire specialists. There is a need for user-friendly erosion modelling support that can rapidly incorporate road networks into post-fire analysis.

5 | CONCLUSIONS

The objectives of this study were to evaluate the impacts of two roads on post fire erosion and sediment delivery following the 2016 71-ha Emerald Fire in the Lake Tahoe Basin, USA; to appraise the utility of the ERMiT and WEPP models for post fire erosion estimates, and to identify advanced GIS methods that can assist in meeting the first two objectives that can be applied to other post-fire landscapes.

GIS surface hydrology methods were developed using the flowpath function with different DEM resolutions, and different critical source areas to evaluate the effect of roads on overland flow. In addition, two types of landscape belt analysis were applied to evaluate the effects of the roads on surface hydrology. We found that the number of flow paths below a road can be up to 50% less than above the road, and that flow path lengths can be reduced by more than 75% due to road networks. We estimated erosion by 2-m pixel based on landscape position, pixel slope and wildfire burn severity through a

GIS-based soil erosion model and high-resolution LiDAR terrain data. Interfaces to the WEPP model including the ERMiT post fire interface, GeoWEPP, the ArcMap application, and the WEPP Windows hillslope and watershed applications were all used to support the erosion analysis. Fire greatly increased the soil erosion risk with estimated erosion rates greater than 4 Mg ha^{-1} $year^{-1}$ for nearly 80% of the burned area. The model predictions conformed well with reported sediment depositions immediately following the fire, confirming that the WEPP technology provided reasonable erosion estimates. The study also confirmed that sediment deposition is more likely on roads with gradients less than 5%. The modelling showed that even though roads are generally thought to exacerbate erosion problems on forested landscapes, in the post-fire environment they had complex and variable effects on runoff and sediment transport. Overall, the road surfaces and road sediment detention basins created opportunities to catch a considerable amount of sediment. In some cases, the roads diverted upland runoff and sediment to the adjacent sub-catchment. The road fillslopes were predicted to be at risk for high onsite soil loss. The modelling and onsite observations suggest that low gradient roads are preferable for minimizing sediment delivery, and on steeper gradients, a road drain system including well-spaced culverts with energy dissipating or sediment basin outlets can reduce the likelihood of water and sediment flooding over the road surface and minimize the risk of downstream sediment delivery. Measuring runoff and erosion immediately following wildfire is challenging, but additional field studies evaluating the effects different road designs, gradients, culvert spacings and sediment basins immediately post fire are needed. Results of such studies would aid forest road planners and watershed managers to design and maintain road networks to minimize sediment delivery from both undisturbed and burned forest landscapes.

ACKNOWLEDGEMENTS

This study was supported by the USDA Forest Service Pacific Southwest Research Station, using funds provided by the Bureau of Land Management through the sale of public lands as authorized by the Southern Nevada Public Land Management Act, USA. It was also supported by the National Natural Science Foundation of China (Project 41571273 and 41807077), and the China Scholarship Council (Project 201604910077). The authors acknowledge the assistance in onsite data collection by Ina Sue Miller, a Hydrologist with the USDA Forest Service Rocky Mountain Research Station, Moscow, Idaho, USA.

CONFLICT OF INTEREST

The authors declare no conflicts of interest.

DATA AVAILABILITY STATEMENT

The data that support the findings of this study are available from the corresponding author upon reasonable request.

ORCID

William Elliot https://orcid.org/0000-0002-3792-3058

REFERENCES

Ackerman, E. A. (1941). The Köppen classification of climates in North America. *Geographical Review*, *31*(1), 105–111.

Akay, A. E., Erdas, O., Reis, M., & Yuksel, A. (2008). Estimating sediment yield from a forest road network by using a sediment prediction model and GIS techniques. *Building and Environment*, *43*, 687–695. https://doi.org/10.1016/j.buildenv.2007.01.047

Andrews, P. L.(2018). *The Rothermel surface fire spread model and associated developments: A comprehensive explanation. Gen. Tech. Rep. RMRS-GTR-371*. (1–121). Fort Collins, CO: U.S. Department of Agriculture, Forest Service, Rocky Mountain Research Station. https://www.fs.usda.gov/treesearch/pubs/55928.

Araujo, H. A., Page, A., Cooper, A. B., Venditti, J., MacIsaac, E., Hassan, M. A., & Knowler, D. (2014). Modelling changes in suspended sediment from forest road surfaces in a coastal watershed of British Columbia. *Hydrological Processes*, *28*, 4914–4927. https://doi.org/10.1002/hyp.9989

Boll, J., Brooks, E. S., Crabtree, B., Dun, S., & Steenhuis, T. A. (2015). Variable source area hydrology modeling with the water erosion prediction project model. *Journal of the American Water Resources Association*, *52*(2), 330–342. https://doi.org/10.1111/1752-1688.12294

Breiman, L. (2001). Random forests. *Machine Learning*, *45*, 5–32.

Brooks, E. S., Boll, J., Elliot, W. J., & Dechert, T. (2006). Global Positioning System/GIS-based approach for modeling erosion from large road networks. *Journal of Hydrologic Engineering*, *11*, 418–426. https://doi.org/10.1061/(ASCE)1084-0699(2006)11:5(418)

Brooks, E. S., Dobre, M., Elliot, W. J., Wu, J. Q., & Boll, J. (2016). Watershed-scale evaluation of the Water Erosion Prediction Project (WEPP) model in the Lake Tahoe basin. *Journal of Hydrology*, *533*, 389–402. https://doi.org/10.1016/j.jhydrol.2015.12.004

Cao, L. X., Wang, Y., & Liu, C. (2021). Study of unpaved road surface erosion based on terrestrial laser scanning. *CATENA*, *199*, 105091. https://doi.org/10.1016/j.catena.2020.105091

Cerdà, A., & Lasanta, A. (2005). Long-term erosional responses after fire in the Central Spanish Pyrenees: 1. Water and sediment yield. *CATENA*, *60*, 59–80. https://doi.org/10.1016/j.catena.2004.09.006

Coats, R., Larsen, M., Heyvaert, A., Thomas, J., Luck, M., & Reuter, J. (2008). Nutrient and sediment production, watershed characteristics, and land use in the Tahoe Basin, California-Nevada. *Journal of the American Water Resources Association*, *44*, 754–770. https://doi.org/10.1111/j.1752-1688.2008.00203.x

Cole, R. P., Bladon, K. D., Wagenbrenner, J. W., & Coe, B. R. (2020). Hillslope sediment production after wildfire and post-fire forest management in northern California. *Hydrological Processes*, *2020*(42), 5242–5259. https://doi.org/10.1002/hyp.13932

Cornish, P. M. (2001). The effects of roading, harvesting and forest regeneration on streamwater turbidity levels in a moist eucalypt forest. *Forest Ecology and Management*, *152*, 293–312. https://doi.org/10.1016/S0378-1127(00)00611-3

Croke, J., & Mockler, S. (2001). Gully initiation and road-to-stream linkage in a forested catchment, southeastern Australia. *Earth Surface Processes and Landforms*, *26*, 205–217. https://doi.org/10.1002/1096-9837(200102)26:2<205:AID-ESP168>3.0.CO;2-G

Croke, J., Mockler, S., Fogarty, P., & Takken, I. (2005). Sediment concentration changes in runoff pathways from a forest road network and the resultant spatial pattern of catchment connectivity. *Geomorphology*, *68*, 257–268. https://doi.org/10.1016/j.geomorph.2004.11.020

Cuo, L., Giambelluca, T. W., Ziegler, A. D., & Nullet, M. A. (2008). The roles of roads and agricultural land use in altering hydrological processes in Nam Mae Rim watershed, northern Thailand. *Hydrological Processes*, *22*(22), 4339–4354.

DeBano, L. F. (2000). The role of fire and soil heating on water repellency in wildland environments: A review. *Journal of Hydrology*, *231–232*, 195–206. https://doi.org/10.1016/S0022-1694(00)00194-3

DeBano, L. F., Neary, D., & Ffolliott, P. (1998). *Fire's effects on ecosystems* (p. 352). John Wiley & Sons.

Doerr, S. H., Shakesby, R. A., & Walsh, R. P. D. (2000). Soil water repellency: Its causes, characteristics and hydro-geomorphological significance. *Earth Science Reviews*, *51*, 33–65. https://doi.org/10.1016/S0012-8252(00)00011-8

Dun, S., Wu, J. Q., Elliot, W. J., Robichaud, P. R., Flanagan, D. C., Frankenberger, J. R., Brown, R. E., & Xu, A. C. (2009). Adapting the Water Erosion Prediction Project (WEPP) model for forest applications. *Journal of Hydrology*, *366*(2009), 46–54.

Ebel, B. A. (2012). Wildfire impacts on soil-water retention in the Colorado Front Range, United States. *Water Resources Research*, *48*, W12515. https://doi.org/10.1029/2012WR012362

Elliot, W. J. (2004). WEPP Internet interfaces for forest erosion prediction. *Journal of the American Water Resources Association*, *40*, 299–309. https://doi.org/10.1111/j.1752-1688.2004.tb01030.x

Elliot, W. J. (2013). Erosion processes and prediction with WEPP technology in forests in the Northwestern U.S. *Transactions of the ASABE*, *56*, 563–579. https://doi.org/10.13031/2013.42680

Elliot, W. J., Cao, L., Long, J. W., Dobre, M., Lew, R., & Miller, M. E. (2018). Estimates of surface and mass erosion following the 2016 Emerald Wildfire, Final Report to the Late Tahoe West Shore Restoration Project. p. 27. Retrieved from https://www.fs.fed.us/psw/partnerships/tahoescience/p101_elliot.shtml

Elliot, W. J., & Hall, D. E. (2010). Disturbed WEPP Model 2.0. Ver. 2014.04.14. Moscow, ID: U.S. Department of Agriculture, Forest Service, Rocky Mountain Research Station. Retrieved from https://forest.moscowfsl.wsu.edu/fswepp/

Elliot, W. J., Hall, D. E., & Scheele D. L. (2000). Disturbed WEPP (Draft 02/2000) WEPP interface for disturbed forest and range runoff, erosion and sediment delivery, Technical Documentation. Retrieved from https://forest.moscowfsl.wsu.edu/fswepp/docs/distweppdoc.html

Elliot, W. J., Miller, I. S., & Cao, L. (2018). *Results of erosion analysis of the Clear Creek road network, Nez Perce-Clearwater National Forest* (pp. 15). U.S. Department of Agriculture, Forest Service Rocky Mountain Research Station. Retrieved from https://www.fs.usda.gov/rmrs/sites/default/files/documents/Clear_Creek_Road_Analysis_Report.pdf

Elliot, W. J., Miller, M. E., & Enstice, N. (2016). Targeting forest management through fire and erosion modeling. *International Journal of Wildland Fire*, *25*, 876–887. https://doi.org/10.1071/WF15007

Elliot, W. J., & Tysdal, L. N. (1999). Understanding and reducing erosion from insloping roads. *Journal of Forestry*, *97*(8), 30–34.

Environmental Systems Research Institute (ESRI). (2016). *Buffer*. Retrieved from https://desktop.arcgis.com/en/arcmap/10.3/tools/analysis-toolbox/buffer.htm

Feikema, P. M., Sheridan, G. J., Argent, R. M., Lane, P. N. J., & Grayson, R. B. (2011). Estimating catchment-scale impacts of wildfire on sediment and nutrient loads using the E2 catchment modelling framework. *Environmental Modelling & Software*, *26*, 913–928.

Finkner, S. C., Nearing, M. A., Foster, G. R., & Gilley, J. E. (1989). A simplified equation for modeling sediment transport capacity. *Transactions of the ASAE*, *32*, 1545–1550. https://doi.org/10.13031/2013.31187

Flanagan, D. C., Frankenberger, J. R., Cochrane, T. A., Renschler, C. S., & Elliot, W. J. (2013). Geospatial application of the Water Erosion Prediction Project (WEPP) model. *Transactions of the ASABE*, *56*, 591–601. https://doi.org/10.13031/2013.42681

Flanagan, D. C., & Livingston, S. J., eds. 1995. *WEPP user summary*. NSERL Report No. 11. West Lafayette, IN: USDA-ARS National Soil Erosion Research Laboratory, p. 141. Retrieved from https://www.ars.usda.gov/ARSUserFiles/50201000/WEPP/usersum.pdf

Flanagan, D.C., & Nearing, M. A., eds. (1995). *USDA – Water Erosion Prediction Project hillslope profile and watershed model documentation*. NSERL Report No. 10. West Lafayette, IN: USDA-ARS National Soil Erosion Research Laboratory. Retrieved from https://www.ars.usda.gov/midwest-area/west-lafayette-in/national-soil-erosion-research/docs/wepp/wepp-model-documentation/

Foltz, R. B., Robichaud, P. R., & Rhee, H. (2009). A synthesis of post-fire road treatments for BAER teams: Methods, treatment effectiveness, and decision-making tools for rehabilitation. *General Technical Report RMRS-GTR-228*. (p. 152) Fort Collins, CO: U.S. Department of Agriculture, Forest Service, Rocky Mountain Research Station.

Grace, J. M., III. (2017). Predicting forest road surface erosion and storm runoff from high-elevation sites. *Transactions of the ASABE*, *60*, 705–719. https://doi.org/10.13031/trans.11646

Greenbaum, N., Wittenberg, L., Malkinson, D., & Inbar, M. (2020). Hydrological and sedimentological changes following the 2010-forest fire in the Nahal Oren Basin, Mt. Carmel Israel–a comparison to pre-fire natural rates. *CATENA*, *196*, 104891. https://doi.org/10.1016/j.catena.2020.104891

Gucinski, H., Furniss, M. J., Ziemer, R. R., & Brookes, M. H. (2001). Forest roads: A synthesis of scientific information. *General Technical Report PNWGTR-509* (pp. 103). Portland, OR: U.S. Department of Agriculture, Forest Service, Pacific Northwest Research Station.

Johnson, D. W., Fenn, M. E., Miller, W. W., & Hunsaker, C. F. (2009). Fire effects on carbon and nitrogen cycling in forests of the Sierra Nevada. In *Developments in environmental science* (Vol. 8, pp. 405–423), chap. 18. The Netherlands: Elsevier. Retrieved from https://www.fs.fed.us/psw/pubs/34233

Jones, J. A., & Grant, G. E. (1996). Peak flow responses to clear-cutting and roads in small and large basins, western Cascades, Oregon. *Water Resources Research*, *32*, 959–974. https://doi.org/10.1029/95WR03493

Katz, H. A., Daniels, J. M., & Ryan, S. (2014). Slope-area thresholds of road-induced gully erosion and consequent hillslope-channel interactions. *Earth Surface Processes and Landforms*, *39*, 285–295.

Kumar, M., Sheikh, M. A., Bhat, J. A., & Bussmann, R. W. (2013). Effect of fire on soil nutrients and under story vegetation in Chir pine forest in Garhwal Himalaya, India. *Acta Ecologica Sinica*, *33*, 59–63. https://doi.org/10.1016/j.chnaes.2012.11.001

Laflen, J. M., Elliot, W. J., Flanagan, D. C., Meyer, C. R., & Nearing, M. A. (1997). WEPP: Predicting water erosion using a process-based model. *Journal of Soil and Water Conservation*, *52*(2), 96–102.

Laflen, J. M., Flanagan, D. C., & Engel, B. A. (2001, January 3–5). Application of WEPP to construction sites. (pp 135–138). In Ascough, II, J. C., & Flanagan, D. C. (eds.). *Soil Erosion Research for the 21st Century, Proc. Int Symp*., Honolulu, HI. St. Joseph, MI: American Society of Agricultural Engineers.

Lane, P. N. J., Hairsine, P. B., Croke, J. C., & Takken, I. (2006). Quantifying diffuse pathways for overland flow between the roads and streams of the mountain ash forests of central Victoria Australia. *Hydrological Processes*, *20*, 1875–1884. https://doi.org/10.1002/hyp.5940

Larson-Nash, S. S., Robichaud, P. R., Pierson, F. B., Moffet, C. A., Williams, C. J., Spaeth, K. E., Brown, R. E., & Lewis, S. A. (2018). Recovery of small-scale infiltration and erosion after wildfires. *Journal of Hydrology and Hydromechanics*, *66*(3), 261–270.

Lew, R. Dobre, M., Elliot, W., Robichaud, P., Brooks, E., Srivastava, A., & Frakenberger, J. (2020). WEPP cloud: Lake Tahoe. Retrieved from https://wepp1.nkn.uidaho.edu/weppcloud/lt/

Li, X., Jin, H., Wang, H., Wu, X., Huang, Y., He, R., Luo, D., & Jin, X. (2020). Distributive features of soil carbon and nutrients in permafrost regions affected by forest fires in northern Da Xing'anling (Hinggan) Mountains, NE China. *CATENA*, *185*, 104304. https://doi.org/10.1016/j.catena.2019.104304

Liu, X., Wu, J. Q., Conrad, P. W., Dun, S., Todd, C. S., McNearny, R. L., Elliot, W. J., Rhee, H., & Clark, P. (2015). Impact of surface coal mining on soil hydraulic properties. *Transactions of the Society for Mining, Metallurgy and Exploration*, *338*, 381–392.

Lopes A. R., Girona-García A., Corticeiro S., Martins R., Keizer J. J., Vieira D. C. S. (2021). What is wrong with post-fire soil erosion modelling? A meta-analysis on current approaches, research gaps, and future directions. *Earth Surface Processes and Landforms*, *46*(1), 205–219. http://dx.doi.org/10.1002/esp.5020.

Luce, C., & Black, T. (1999). Sediment production from forest roads in western Oregon. *Water Resources Research*, *35*, 2561–2570. https://doi.org/10.1029/1999WR900135

MacDonald, L. H., & Coe, D. B. R. (2008). Road sediment production and delivery: Processes and management. In *Proceedings of the first world landslide forum, international Programme on landslides and international strategy for disaster reduction* (pp. 381–384). Tokyo, Japan: United Nations University.

McCormick, F. H., Riemen, B. E., & Kershner, J. L. (2010). Biological responses to stressors in aquatic ecosystems in Western North America: Cumulative watershed effects of fuel treatments, wildfire, and post-wildfire remediation. In W. J. Elliot, I. S. Miller, & L. Audin (Eds.), *Cumulative watershed effects of fuel management in the Western United States. General Technical Report RMRS-GTR-231* (pp. 206–233). Fort Collins, CO: U.S. Department of Agriculture, Forest Service, Rocky Mountain Research Station, chap. 11.

Miller, M. E., Billmire, M., & Banach, D. (2015). *NASA BAER user manual for running GeoWEPP* (p. 21). Michigan Technological Research Institute. Retrieved from http://geodjango.mtri.org/geowepp/

Miller, M. E., Elliot, W. J., Billmire, M., Robichaud, P. R., & Endsley, K. A. (2016). Rapid response tools and datasets for post-fire remediation: Linking remote sensing and process-based hydrologic models. *International Journal of Wildland Fire*, *25*, 1061–1073. https://doi.org/10.1071/WF15162

Miller, M. E., MacDonald, L. H., Robichaud, P. R., & Elliot, W. J. (2011). Predicting post-fire hillslope erosion in forest lands of the western United States. *International Journal of Wildland Fire*, *20*, 982–999. https://doi.org/10.1071/WF09142

Milller, M. E., Billmire, M., Elliot, W., Robichaud, P., & Miller, S. (2019). *NASA RRED user manual for running QWEPP* (p. 13). Michigan Technological Research Institute. Retrieved from http://rred.mtri.org/baer/static/RRED_user_manual_for_QGIS.pdf

Moody, J. A., Ebel, B. A., Nyman, P., Martin, D. A., Stoof, C. R., & McKinley, R. (2016). Relations between soil hydraulic properties and burn severity. *International Journal of Wildland Fire*, *25*, 279–293.

Moody, J. A., Shakesby, R. A., Robichaud, P. R., Cannon, S. H., & Martin, D. A. (2013). Current research issues related to post-wildfire runoff and erosion processes. *Earth-Science Reviews*, *122*, 10–37. https://doi.org/10.1016/j.earscirev.2013.03.004

Motha, J. A., Wallbrink, P. J., Hairsine, P. B., & Grayson, R. B. (2003). Determining the sources of suspended sediment in a forested catchment in southeastern Australia. (pp 14). *Water Resources Research*, *39*, 1056. https://doi.org/10.1029/2001WR000794

Napper, C. (2006). *Burned area emergency response treatments catalogue. 0625 1801-SDTDC* (p. 266). USDA Forest Service, Sand Dimas Technology and Development Center.

Nash, J. E., & Sutcliffe, J. V. (1970). River flow forecasting through conceptual models. *Journal of Hydrology*, *10*, 282–290.

Natural Resources Conservation Service (NRCS). 2020. National Water Climate Center, Echo Peak SnoTel Site. Retrieved from https://wcc.sc.egov.usda.gov/nwcc/site?sitenum=463

Nearing, M. A., Liu, B. Y., Risse, L. M., & Zhang, X. (1996). Curve numbers and Green-Ampt effective hydraulic conductivities. *Water Resources Bulletin*, *32*(1), 125–136.

Nevada Division of Environmental Protection (NDEP). (2011). *Final Lake Tahoe total maximum daily load* (p. 339). Carson City, NV. Retrieved from https://archive.epa.gov/region09/water/archive/watershed/tahoe/pdf/final-lake-tahoe-tmdl.pdf

Nunes, J. P., Quintanilla, P. N., Santos, J. M., Serpa, D., Carvalho-Santos, C., Rocha, J., Keizer, J. J., & Keestra, S. D. (2018). Afforestation, subsequent forest fires and provision of hydrological services: A model-based analysis for a Mediterranean mountainous catchment. *Land Degradation and Development*, *29*(3), 776–788. https://doi.org/10.1002/ldr.2776

Nyman, P., & Moody, J. A. (2012). Variations in soil detachment rates after wildfire as a function of soil depth, flow properties and root properties. In *Scientific Investigations Report 2012-5233*. Reston, VA: U.S. Department of Interior, U.S. Geological Survey.

Owens, P. N., Giles, T. R., Petticrew, E. L., Leggat, M. S., Moore, R. D., & Eaton, B. C. (2013). Muted responses of streamflow and suspended sediment flux in a wildfire-affected watershed. *Geomorphology*, *202*, 128–139. https://doi.org/10.1016/j.geomorph.2013.01.001

Parsakhoo, A., Lotfalian, M., Kavian, A., & Hosseini, S. A. (2014). Prediction of the soil erosion in a forest and sediment yield from road network through GIS and SEDMODL. *International Journal of Sediment Research*, *29*, 118–125. https://doi.org/10.1016/S1001-6279(14)60027-5

Parsons, A., Robichaud, P. R., Lewis, S. A., Napper, C., & Clark, J. T. (2010). Field guide for mapping post-fire soil burn severity. In *General Technical Report RMRS-GTR-243* (p. 49). Fort Collins, CO: Rocky Mountain Research Station.

Persendt, F. C., & Gomez, C. (2016). Assessment of drainage network extractions in a low-relief area of the Cuvelai Basin (Namibia) from multiple sources: LiDAR, topographic maps, and digital aerial orthophotographs. *Geomorphology*, *260*, 32–50. https://doi.org/10.1016/j.geomorph.2015.06.047

Pierson, F. B., Robichaud, P. R., Moffet, C. A., Spaeth, K. E., Williams, C. J., Hardegree, S. P., & Clark, P. E. (2008). Soil water repellency and infiltration in coarse-textured soils of burned and unburned sagebrush ecosystems. *CATENA*, *74*(2), 98–108.

Quinn, D. S. (2018). *Simulation of post-fire watershed hydrology and erosion responses with the physically based WEPP model* (M.S. thesis). Moscow, ID: University of Idaho, p. 85.

Ramos-Scharrón, C. E., & MacDonald, L. H. (2005). Measurement and prediction of sediment production from unpaved roads, St John, US Virgin Islands. *Earth Surface Processes and Landforms*, *30*, 1283–1304. https://doi.org/10.1002/esp.1201

Reid, L. M. (2010). Cumulative effects of fuel treatments on channel erosion and mass wasting. In W. J. Elliot, I. S. Miller, & L. Audin (Eds.), *cumulative watershed effects of fuel management in the Western United States. General Technical Report RMRS-GTR-231* (pp. 101–125). Fort Collins, CO: U.S. Department of Agriculture, Forest Service, Rocky Mountain Research Station, chap. 10.

Robichaud, P. R. (2005). Measurement of post-fire hillslope erosion to evaluate and model rehabilitation treatment effectiveness and recovery. *International Journal of Wildland Fire*, *14*, 475–485. https://doi.org/10.1071/WF05031

Robichaud, P. R., Beyers, J. L., & Neary, D. G. (2000). Evaluating the effectiveness of postfire rehabilitation treatments. In *General Technical Report RMRS-GTR-63* (p. 85). Fort Collins, CO: U.S. Department of Agriculture, Forest Service, Rocky Mountain Research Station.

Robichaud, P. R., Bone, E. D., Lewis, S. A., Brooks, E. S., & Brown, R. E. (2020). Effectiveness of post-fire salvage logging stream buffer management for hillslope erosion in the U.S. Inland Northwest Mountains. *Hydrological Processes*, *35*, e13943.

Robichaud, P. R., Elliot, W. J., Lewis, S. A., & Miller, M. E. (2016). Validation of a probabilistic post-fire erosion model. *International Journal of Wildland Fire*, *2016*(25), 337–350. https://doi.org/10.1071/WF14171

Robichaud, P. R., Elliot, W. J., Pierson, F. B., Hall, D. E., & Moffet, C. A. (2007). Predicting postfire erosion and mitigation effectiveness with a web-based probabilistic erosion model. *CATENA*, *71*, 229–241. https://doi.org/10.1016/j.catena.2007.03.003

Robichaud, P. R., Lewis, S. A., Laes, D. Y. M., Hudak, A. T., Kokaly, R. F., & Zamudio, J. A. (2007). Postfire soil burn severity mapping with hyperspectral image umixing. *Remote Sensing of Environment*, *108*, 467–480.

Robichaud, P. R., Storrar, K. A., & Wagenbrenner, J. W. (2019). Effectiveness of straw bale check dams at reducing post-fire sediment yields from steep ephemeral channels. *Science of the Total Environment*, *676*, 721–731. https://doi.org/10.1016/j.scitotenv.2019.04.246

Robichaud, P. R., Wagenbrenner, J. W., & Brown, R. E. (2010). Rill erosion in natural and disturbed forests: 1. Measurements. *Water Resources Research*, *46*, W10506. https://doi.org/10.1029/2009WR008314

Robichaud, P. R., Wagenbrenner, J. W., Pierson, F. B., Spaeth, K. E., Ashmun, L. E., & Moffet, C. A. (2016). Infiltration and interrill erosion rates after wildfire in western Montana, USA. *CATENA*, *142*(20160), 77–88.

Scheele, D. L., Elliot, W. J., & Hall, D. E. (2001). Enhancements to the CLIGEN weather generator for mountainous or custom applications (pp. 392-395). ASAE Pub. No. 701P0007. Presented January 3-5, 2000, Honolulu, HI. In J. C. Ashough, II & D. C. Flanagan (Eds.), *Soil erosion for the 21st century: Proceedings of the International Symposium*. St. Joseph, MI: ASAE.

Shakesby, R., Moody, J., Martin, D., & Robichaud, P. (2016). Synthesizing empirical results to improve predictions of post-wildfire runoff and erosion response. *International Journal of Wildland Fire*, *25*(3), 257–261. https://doi.org/10.1071/WF16021

Sheridan, G. J., Lane, P. N. J., & Noske, P. J. (2007). Quantification of hillslope runoff and erosion processes before and after wildfire in a wet Eucalyptus forest. *Journal of Hydrology*, *343*(1–2), 12–28. https://doi.org/10.1016/j.jhydrol.2007.06.005

Sheridan, G. J., & Noske, P. J. (2007). Catchment-scale contribution of forest roads to stream exports of sediment, phosphorus and nitrogen. *Hydrological Processes*, *21*, 3107–3122. https://doi.org/10.1002/hyp.6531

Sidle, R. C., Sasaki, S., Otsuki, M., Noguchi, S., & Nik, A. R. (2004). Sediment pathways in a tropical forest: Effects of logging roads and skid trails. *Hydrological Processes*, *18*, 703–720. https://doi.org/10.1002/hyp.1364

Smith, H. G., Sheridan, G. J., Lane, P. N. J., Nyman, P., & Haydon, S. (2011). Wildfire effects on water quality in forest catchments: A review with implications for water supply. *Journal of Hydrology*, *396*, 170–192. https://doi.org/10.1016/j.jhydrol.2010.10.043

Sosa-Pérez, G., & MacDonald, L. H. (2017). Wildfire effects on road surface erosion, deposition, and road–stream connectivity. *Earth Surface Processes and Landforms*, *42*, 735–748. https://doi.org/10.1002/esp.4018

Soulis, K. X., Dercas, N., & Papadaki, C. H. (2014). Effects of forest roads on the hydrological response of a small-scale mountain watershed in Greece. *Hydrological Processes*, *29*, 1772–1782. https://doi.org/10.1002/hyp.10301

Srivastava, A., Brooks, E. S., Dobre, M., Elliot, W. J., Wu, J. Q., Flanagan, D. C., Gravelle, J. A., & Link, T. E. (2020). Modeling forest management effects on water and sediment yield from nested, paired watersheds in the interior Pacific Northwest USA using WEPP. *Science of the Total Environment*, *701*, 134877. https://doi.org/10.1016/j.scitotenv.2019.134877

Srivastava, A., Dobre, M., Wu, J. Q., Elliot, W. J., Bruner, E. A., Dun, S., Brooks, E. S., & Miller, I. S. (2013). Modifying WEPP to improve streamflow simulation in a Pacific Northwest watershed. *Transactions of the American Society of Agricultural and Biological Engineers*, *56*(2), 603–611.

Srivastava, A., Wu, J. Q., Elliot, W. J., Brooks, E. S., & Flanagan, D. C. (2017). Modeling streamflow in a snow-dominated forest watershed using the Water Erosion Prediction Project (WEPP) model. *Transactions of the American Society of Agricultural and Biological Engineers*, *60*(4), 1171–1187.

Srivastava, A., Wu, J. Q., Elliot, W. J., Brooks, E. S., & Flanagan, D. C. (2018). A simulation study to estimate effects of wildfire and forest management on hydrology and sediment in a forested watershed, Northwestern U.S. *Transactions of the American Society of Agricultural and Biological Engineers*, *61*(5), 1579–1601.

Stavi, I., Barkai, D., Knoll, Y. M., Glion, H. A., Katra, I., Brook, A., & Zaady, E. (2017). Fire impact on soil-water repellency and functioning of semi-arid croplands and rangelands: Implications for prescribed burnings and wildfires. *Geomorphology*, *280*, 67–75. https://doi.org/10.1016/j.geomorph.2016.12.015

Takken, I., Croke, J., & Lane, P. (2008). Thresholds for channel initiation at road drain outlets. *CATENA*, *75*, 257–267. https://doi.org/10.1016/j.catena.2008.07.001

Tarboton, D. G., Bras, R. L., & Rodriguez-Iturbe, I. (1991). On the extraction of channel networks from digital elevation data. *Hydrological Processes*, *5*, 81–100.

Thomaz, E. L., Vestena, L. R., & Ramos Scharrón, C. E. (2014). The effects of unpaved roads on suspended sediment concentration at varying spatial scales – A case study from Southern Brazil. *Water and Environment Journal*, *28*, 547–555. https://doi.org/10.1111/wej.12070

United States Department of Agriculture, Natural Resources Conservation Service (USDA). 2007. *Soil survey of the Tahoe Basin Area, California and Nevada*. Retrieved from Washington, D.C.: USDA Natural Resource Conservation Service. http://soils.usda.gov/survey/printed_surveys/

Vieira, D., Prats, S., Nunes, J., Shakesby, R., Coelho, C., & Keizer, J. (2014). Modelling runoff and erosion, and their mitigation, in burned Portuguese forest using the revised Morgan-Morgan-Finney model. *Forest Ecology and Management*, *314*, 150–165. https://doi.org/10.1016/j.foreco.2013.12.006

Vollmer, M. (2016). Emerald fire update. Presentation to Tahoe Regional Planning Authority Advisory Planning Commission on 8 November 2016.

Wagenbrenner, J. W., Robichaud, P. R., & Brown, R. E. (2016). Rill erosion in burned and salvage logged western montane forests: Effects of logging equipment type, traffic level, and slash treatment. *Journal of Hydrology*, *541*, 889–901.

Water Boards and NDEP. (2008). *Lake Tahoe TMDL Pollutant Reduction Opportunity Report* (p. 279). Retrieved from https://www.waterboards.ca.gov/rwqcb6/water_issues/programs/tmdl/lake_tahoe/docs/presentations/pro_report_v2.pdf

Wemple, B. C., Clark, G. E., Ross, D. S., & Rizzo, D. M. (2017). Identifying the spatial pattern and importance of hydro-geomorphic drainage impairments on unpaved roads in the northeastern USA. *Earth Surface Processes and Landforms*, *42*, 1652–1665. https://doi.org/10.1002/esp.4113

Wemple, B. C., Jones, J. A., & Grant, G. E. (1996). Channel network extension by logging roads in two basins, western Cascades, Oregon. *Water Resources Bulletin*, *32*, 1195–1207. https://doi.org/10.1111/j.1752-1688.1996.tb03490.x

Wemple, B. C., Swanson, F. J., & Jones, J. A. (2001). Forest roads and geomorphic process interactions, Cascade Range, Oregon. *Earth Surface Processes and Landforms*, *26*, 191–204. https://doi.org/10.1002/1096-9837(200102)26:2<191::AID-ESP175>3.0.CO;2-U

Yang, P., Ames, D. P., Fonseca, A., Anderson, D., Shrestha, R., Glenn, N. F., & Cao, Y. (2014). What is the effect of LiDAR-derived DEM resolution on large-scale watershed model results? *Environmental Modelling & Software*, *58*, 48–57. https://doi.org/10.1016/j.envsoft.2014.04.005

Young, D. (2016). *BAER assessment soils report – Emerald Fire* (p. 13). Redding, CA: U.S. Department of Agriculture, Forest Service, Region 5, Shasta-Trinity National Forest.

Zhai, X., Zhang, Y., Wang, X., Xia, J., & Liang, T. (2014). Non-point source pollution modelling using Soil and Water Assessment Tool and its parameter sensitivity analysis in Xin'anjiang catchment, China. *Hydrological Processes*, *28*(4), 1627–1640. https://doi.org/10.1002/hyp.9688

Zhang, J. X., Wu, J. Q., Chang, K., Elliot, W. J., & Dun, S. (2009). Effects of DEM source and resolution on WEPP hydrologic and erosion simulation: A case study of two forest watersheds in Northern Idaho. *Transactions of the American Society of Agricultural and Biological Engineers*, *52*(2), 447–457.

Zhang, Y., Zhao, Y., Liu, B., Want, Z., & Zhang, S. (2019). Rill and gully erosion on unpaved roads under heavy rainfall in agrcultural watersheds on China's Loess Plateau. *Agriculture, Ecosystems & Environment*, *284*. 1–10. https://doi.org/10.1016/j.agee.2019.106580

Ziegler, A. D., Negishi, J. N., Sidle, R. C., Gomi, T., Noguchi, S., & Nik, A. R. (2007). Persistence of road runoff generation in a logged catchment in Peninsular Malaysia. *Earth Surface Processes and Landforms*, *32*(13), 1947–1970. https://doi.org/10.1002/esp.1508

How to cite this article: Cao L, Elliot W, Long JW. Spatial simulation of forest road effects on hydrology and soil erosion after a wildfire. *Hydrological Processes*. 2021;35:e14139. https://doi.org/10.1002/hyp.14139